

CALCIC MYRMEKITE: POSSIBLE EVIDENCE FOR THE INVOLVEMENT OF WATER DURING THE EVOLUTION OF ANDESINE ANORTHOSITE FROM ST-URBAIN, QUEBEC

ROBERT F. DYMEK

Department of Earth and Planetary Sciences and McDonnell Center for the Space Sciences, Washington University, St. Louis, Missouri 63130, U.S.A.

CRAIG M. SCHIFFRIES

Department of Geological Sciences, Harvard University, Cambridge, Massachusetts 02138, U.S.A.

ABSTRACT

Vermicular intergrowths of quartz + plagioclase feldspar are found in andesine anorthosite from the St-Urbain massif, Quebec, where they comprise up to about 1 volume % of individual samples. Such "myrmekite" occurs along plagioclase grain-boundaries of the host anorthosite as bulbous aggregates (up to ~1 mm across) to thin films (~10–100 μm wide). Plagioclase in the myrmekites ranges from An_{62} to An_{92} , with most compositions near An_{80} . In contrast, plagioclase of the host anorthosite is an antiperthite with composition $\text{An}_{40\pm 3}$. Quartz contents of the myrmekites average about 23% by volume. Boundaries between myrmekite and host plagioclase are sharp, across which the change in plagioclase composition is virtually instantaneous. These textural and chemical features suggest that the boundaries represent an arrested reaction-front, where sodic plagioclase was replaced by calcic plagioclase accompanied by precipitation of quartz. Calculation shows that the conversion of An_{40} to An_{80} (conserving Al) yields almost exactly the amount of quartz observed to occur in the myrmekites. We interpret these calcic myrmekites to be the products of corrosive interaction between cumulate plagioclase crystals and a magmatically derived, high-temperature aqueous fluid. This interpretation is consistent with experimental results on plagioclase-fluid equilibria, whereas the sharpness of the myrmekite boundary is consistent with predictions from fluid-infiltration theory. Alternative origins for these myrmekites through cotectic crystallization, exsolution from feldspar, or decomposition of a precursor phase are not considered viable. Ostensibly similar intergrowths occur in other massif anorthosites and also in layered mafic plutons. Thus calcic myrmekite may be a common (but easily overlooked or ignored) feature of anorthositic rocks in general, providing evidence for the presence of aqueous fluids in systems heretofore considered anhydrous.

Keywords: anorthosite, antiperthite, exsolution, fluids, infiltration, myrmekite, plagioclase, replacement, St-Urbain, Quebec.

SOMMAIRE

Une intercroissance vermiculaire de quartz et de plagioclase occupe environ 1% du volume de l'anorthosite à andésine du massif de St-Urbain, au Québec. On trouve ce genre

de myrmékite le long de la bordure des grains de plagioclase, en agrégat bulbeux (1 mm) ou en liseré (entre 10 et 100 μm de largeur). Le plagioclase de l'intercroissance a une composition entre An_{62} et An_{92} , et près de An_{80} dans la plupart des cas. Par contre, le plagioclase de l'anorthosite hôte est une antiperthite de composition $\text{An}_{40\pm 3}$. L'intercroissance contient environ 23% de quartz par volume. L'interface entre le domaine myrmékitique et le plagioclase hôte est franche, le changement en composition du plagioclase étant abrupt. Ces caractéristiques texturales et chimiques font penser que l'interface représente un front de réaction arrêtée, où le plagioclase sodique se fait remplacer par un plagioclase plus calcique, réaction accompagnée par la précipitation du quartz. Un calcul montre que la conversion de An_{40} à An_{80} , avec conservation de l'aluminium, produit presque exactement la quantité de quartz observée. Cette myrmékite calcique résulterait de l'interaction corrosive d'un fluide aqueux d'origine magmatique, à température élevée, avec les cristaux de plagioclase des cumulats. Cette interprétation concorde avec les résultats expérimentaux sur la réaction entre plagioclase et fluide aqueux, tandis que l'interprétation d'un front de réaction concorde avec les prédictions de la théorie de l'infiltration d'un fluide. Une origine de l'intercroissance par cristallisation cotectique, par exsolution d'un feldspath ou par décomposition d'un précurseur ne peut pas être envisagée. Il est probable qu'une intercroissance semblable se trouve dans les autres massifs d'anorthosite ainsi que dans des plutons mafiques stratiformes. Répandue mais pas facilement repérée ou tout simplement ignorée, elle serait un indice de la présence d'un fluide aqueux dans des roches jusqu'ici jugées anhydres.

(Traduit par la Rédaction)

Mots-clés: anorthosite, antiperthite, exsolution, phase fluide, infiltration, myrmékite, plagioclase, remplacement, St-Urbain, Québec.

INTRODUCTION

In 1960, A. F. Buddington proposed that massif anorthosites crystallized from a water-bearing magma of overall "gabbroic anorthosite" composition. His principal reason for invoking a hydrous situation was the experimentally demonstrated shift of

the plagioclase-clinopyroxene cotectic boundary in the system Di-An-Ab toward more feldspathic compositions with increased H₂O-content. Hargraves (1962) developed similar arguments and suggested that outward escape of water accompanied solidification of anorthosite, thereby promoting anatexis of country rocks, which could account for the widespread association of anorthosite with the so-called "charnockite" suite. Yoder (1968a) reviewed various lines of experimental evidence bearing on the petrogenesis of massif-type anorthosites, and also noted that water favors the production of highly feldspathic magmas.

Although there is still no consensus on the subject of parent-magma composition, many investigators (*e.g.*, Ashwal 1982) have subsequently embraced Buddington's idea of gabbroic anorthosite, but little if any definitive evidence has been marshaled in support of a significant role for H₂O in massif anorthosites. In fact, evidence to the contrary is seemingly abundant, as an anhydrous plagioclase-pyroxene-olivine-oxide mineralogy is symptomatic of massif anorthosites in general. Prevailing opinion, as summarized in Morse (1982), is that the parent magma for anorthosite was extremely poor in water.

However, the andesine anorthosite at St-Urbain, Quebec, which is the subject of the present study, contains a variety of features that may be explained as plausible consequences of a water-bearing magma. These include: highly oxidized primary magmatic ilmenite - hematite solid solution, high Fe³⁺ in pyroxene, lack of significant Fe²⁺/Mg variation in silicates, widespread presence of biotite, abundant reverse zoning in plagioclase (even in rocks where plagioclase is but a minor constituent, such as in Fe-Ti oxide ores), and the presence of myrmekitic intergrowths of quartz + calcic plagioclase. The suppression of Fe²⁺/Mg fractionation in silicates may be explained by the magmatic reaction: $2\text{FeO} + \text{H}_2\text{O} = \text{Fe}_2\text{O}_3 + \text{H}_2$ (which should also promote precipitation of Fe₂O₃-rich ilmenite), whereas reverse zoning in plagioclase may reflect the well-documented shift of the plagioclase "melting loop" to more anorthitic compositions under hydrous conditions. Each of these features merits detailed consideration, and possibly has alternative explanations.

In this paper we focus primarily on only one of the above: we report on the textures, bulk compositions and plagioclase compositions of "myrmekites" that are found in the St-Urbain massif, and speculate on their origin through corrosive interaction between cumulate plagioclase crystals and late-stage, high-temperature aqueous fluid. These results are combined with additional data and observations on the anorthosite, in the interest of developing a preliminary model for the emplacement and crystallization history of the St-Urbain massif.

GEOLOGICAL SETTING

The St-Urbain massif is located about 120 km northeast of Quebec City, and is situated within the central high-grade granulite terrane of the Grenville structural province. It is a relatively small, oval pluton (about 15 × 30 km; Fig. 1) composed almost exclusively of anorthositic rocks, predominantly andesine anorthosite of several textural types, with minor leuconorite and a few small Fe-Ti oxide deposits (Mawdsley 1927, Roy *et al.* 1972, Rondot 1979). Available petrological and geochemical data indicate a comagmatic relationship for these lithologies (Gromet & Dymek 1981). In addition, as much as 15% of the massif is underlain by relatively older labradorite anorthosite that is petrologically, geochemically and isotopically distinct from, and apparently not directly related to, the andesine anorthosite (Dymek 1980, Gromet & Dymek 1980). Wherever labradorite anorthosite is found in the massif, it is cut by dykes of the andesine anorthosite (see Fig. 2A in Dymek & Gromet 1984).

In general, the massif lacks penetrative deformation, corona structures and other evidence for significant postmagmatic modification. The border zones (outer 1 km) locally consist of layered or banded rocks enriched in orthopyroxene, Fe-Ti oxide, or both. This "foliation" appears to represent an igneous feature that was accentuated during emplacement of the massif to its present level in the crust (Roy *et al.* 1972; *cf.* Martignole & Schrijver 1970). The country rock includes pyroxene-bearing granitic intrusive rocks of overall quartz monzodiorite composition, banded "charnockitic" gneisses, and a complexly deformed sequence of paragneisses and granites. At one locality near the northwest corner of the massif, a thin (100 m or less) unit of apatite-, ilmenite-, magnetite-rich "norite" (Powell *et al.* 1982) separates anorthosite from country rock. Other oxide-apatite rocks that lack magnetite are associated with the ilmenite orebodies, where they may contain accessory rutile and sapphirine as well as abundant biotite (Dymek 1984).

SAMPLE DESCRIPTION

Data presented in this paper are restricted to samples of andesine anorthosite, the locations of which are shown on Figure 1. One of these (STU 24-7) is the plagioclase-rich host to an extremely coarse-grained anorthosite that contains orthopyroxene megacrysts, which are described in Dymek & Gromet (1984). The remainder of the samples are anorthosites *sensu stricto* (those from "Mont du lac-des-Cygnés" are examples of anorthosite dykes) that consist of more than 95% plagioclase together with small amounts of Fe-Ti oxide (as exsolved lamellar intergrowths with approximate compositions $\text{Ilm}_{88}\text{Hem}_{12}$ and $\text{Ilm}_{30}\text{Hem}_{70}$), clinopyroxene ($\text{Ca}_{45}\text{Mg}_{45}\text{Fe}_{10}$ to

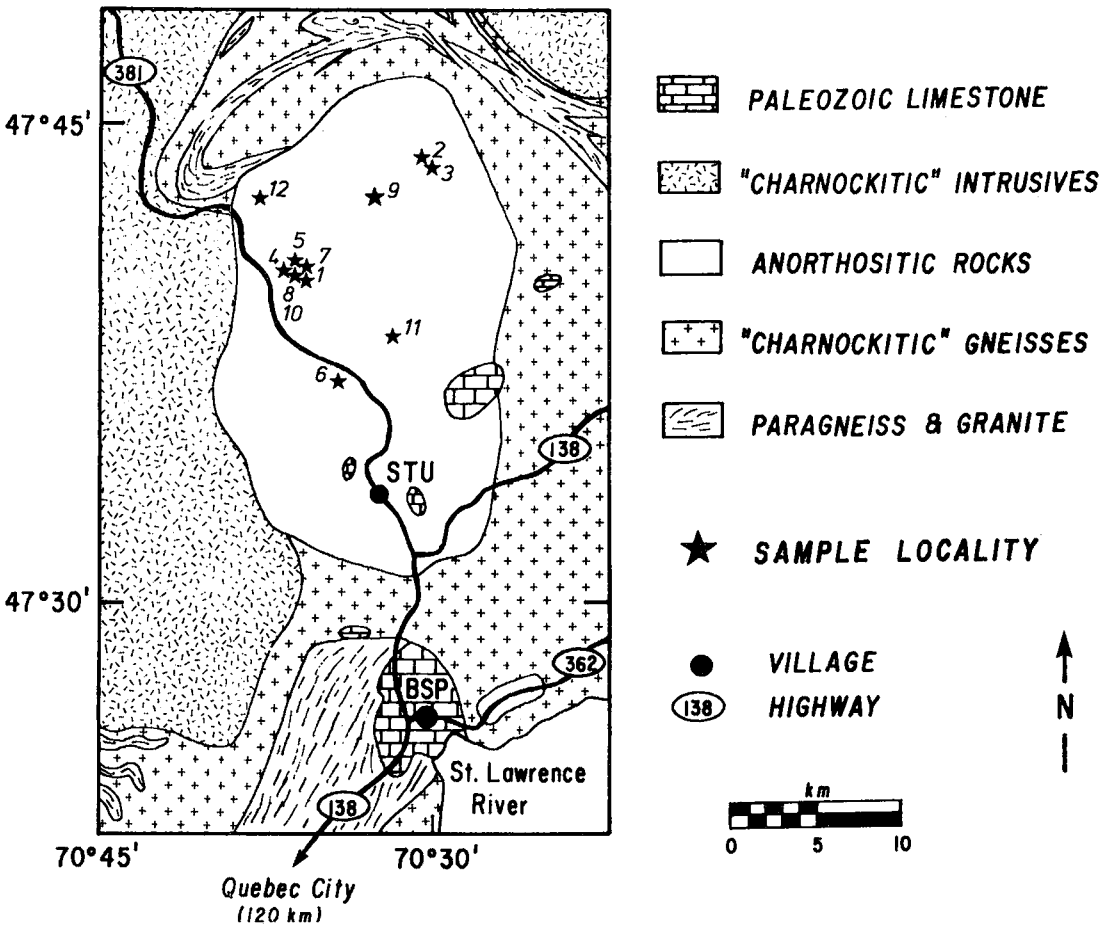


FIG. 1. Simplified regional geology of the St-Urbain area, Charlevoix County, Quebec (adapted from Rondot 1979). Numbered localities correspond to the following samples: 1(Mont du Lac-des-Cygnes: MLC P-368, MLC 20-4, MLC 19-2, MLC 20-3, CHV 80-76); 2(STU 24-19); 3(STU 24-20); 4(STU 22-22); 5(STU 22-25); 6(STU 24-7); 7(STU 22-9, STU 22-11); 8(STU 14-1A); 9(STU 24-18); 10(STU 22-23); 11(STU 25-7); 12(STU 24-21).

$\text{Ca}_{45}\text{Mg}_{40}\text{Fe}_{15}$, orthopyroxene (En_{65-73}), biotite ($X_{\text{Mg}} \sim 0.75-0.85$; $\sim 2-4$ wt. % TiO_2 ; $\sim 1-3$ wt. % F), very rare fluorapatite and, of course "myrmekite", which may constitute up to 1 volume % of a given sample.

In the field, the anorthosites are seen to consist typically of 1-20 cm (locally up to 50 cm) dark blue-grey plagioclase megacrysts set in a finer-grained (typically mm-sized) matrix of pink to pale grey plagioclase. The proportions of megacrysts may vary from 0 to 100% in a given outcrop area, such that the anorthosites range from somewhat homogeneous, medium-grained rocks to very coarse-grained "pegmatitic" types, although grain size seems best characterized as seriate porphyritic. Of particular significance to the present study is the petrographic observation that "myrmekite" appears more promi-

nent in finer-grained materials and in anorthosite dykes.

Factors that control the distribution of plagioclase megacrysts are unclear. Crystal sorting during primary igneous crystallization is suggested by alignment of megacrysts in some dykes. The involvement of igneous processes is supported further by widespread examples of progressive coarsening of grain size into pegmatitic zones where giant crystals of plagioclase, orthopyroxene and Fe-Ti oxide are found commonly with biotite and, rarely, quartz. On the other hand, it is possible that the anorthositic matrix resulted from granulation or recrystallization of megacrysts. In several cases, individual megacrysts appear fractured and seemingly invaded by the matrix. This problem is considered further in the next section.

FELDSPARS OF THE ANDESINE ANORTHOSSITE

Textural characteristics

In thin section, plagioclase exhibits subrounded, polygonal cross-sections, and tabular forms are typically lacking, although some megacrysts are somewhat elongate \perp [010]. Grain boundaries show straight segments, but are highly irregular and even sutured in detail, commonly with interlocking protrusions between adjacent crystals. We see no compelling reasons why such textures could not have resulted from the mutual interference of plagioclase crystals growing from a melt.

All "matrix" grains display well-developed albite and pericline twins, which are curved or bent in some cases. Other features indicative of internal strain include undulose extinction, mosaicism and incipient polygonization. Plagioclase megacrysts are also well-twinned, but exhibit very little evidence of internal strain, although bending of albite twins and minor zones of polygonization have been noted. The latter appear to be localized near pyroxene and oxide inclusions, and are terminated abruptly at megacryst margins.

These observations permit us to address the relationship between megacrysts and matrix plagioclase in a preliminary way. For example, if the finer grain-size of the matrix is a result of deformation and recrystallization of megacrysts, then one would expect this "new" feldspar to be largely strain-free and the "relict" megacrysts to be highly strained, whereas the opposite appears to be the case. Thus we cannot account for grain-size variation in the andesine anorthosite entirely by *in situ* degradation of megacrysts. Moreover, we cannot provide textural evidence for dynamic recrystallization to a finer grain-size, such as that illustrated by Kehlenbeck (1972) for the Lac Rouvry massif.

Nevertheless, it is evident that the feldspar grains experienced some type of deformation, in which the applied stress was accommodated principally by modification of "matrix" plagioclase, with only minor effects on the megacrysts. Whether the resultant strain was induced during movement of a largely consolidated crystal-mush or was related to external forces is unclear, although we prefer the former interpretation.

Plagioclase in the samples studied occurs as antiperthite, and examples of exsolution textures resembling nearly every variety figured by Carstens (1967) from the Egersund (Norway) anorthosite can be found at St-Urbain. The blebs of exsolved alkali feldspar range in shape from rectangular to elliptical to highly elongate, have apparent widths ranging from 1 to 15 μm , and are oriented parallel to several crystallographic directions of the host. The blebs may comprise single sets of parallel arrays, or

multiple sets of intersecting arrays that produce a "Widmanstätten" texture. Contrary to the generalization drawn by Carstens (1967), however, the blebs in the present case are not localized at composition planes of albite twins, but seem to occur at almost any angle to them; they may even lie parallel to the composition planes of pericline twins.

The plagioclase also contains oriented platelets and rodlets of exsolved Fe-Ti oxide (which comprise tiny lamellar hematite-ilmenite intergrowths), and acicular to stubby clinopyroxene (<20 μm long) crystals or crystal aggregates that may also be of exsolution origin. In a few cases, the clinopyroxene aggregates occur with granular Fe-Ti oxide and, rarely, apatite.

At plagioclase grain-boundaries, granular Fe-Ti oxide and subequant to "vermicular" clinopyroxene (both < 100 μm) may be found. These interstitial materials may have crystallized from a trapped melt component.

Chemical compositions

The compositions of plagioclase and alkali feldspar from the andesine anorthosite (Tables 1, 2), together with the compositions of feldspars and other minerals (Tables 4-6), were determined by electron-microprobe analysis using methods outlined in Dymek & Gromet (1984).

Plagioclase compositions are generally within a few mole percent of An_{40} . Individual grains are remarkably homogeneous, with typical compositional variation within any sample being less than 3 mole % An. However, there are important (and not well-understood!) exceptions to this generalization. For example, every boundary with interstitial pyroxene is characterized by a thin (~ 10-50 μm wide) rim of reversely zoned plagioclase. Moreover, every pyroxene inclusion in plagioclase is surrounded by a 10-50- μm wide "halo" of reversely zoned plagioclase. In both situations, compositions as calcic as An_{75} are encountered, K contents of the plagioclase decrease to less 0.05 wt.% K_2O , and both exsolved oxides and alkali feldspar blebs are absent.

The processes leading to the development of reverse zoning may have some bearing on the present problem. Some preliminary interpretations are presented in this report, but a detailed consideration of reverse zoning and its implications will be provided in a subsequent paper (*cf.* Dymek 1981, Dymek & Gromet 1984).

A representative plagioclase composition from each of the 17 samples investigated for this project is listed in Table 1. These data were selected to approximate the mean composition in that specimen, and collectively outline only a small range of overall composition (An_{37} to An_{42}). The values listed for

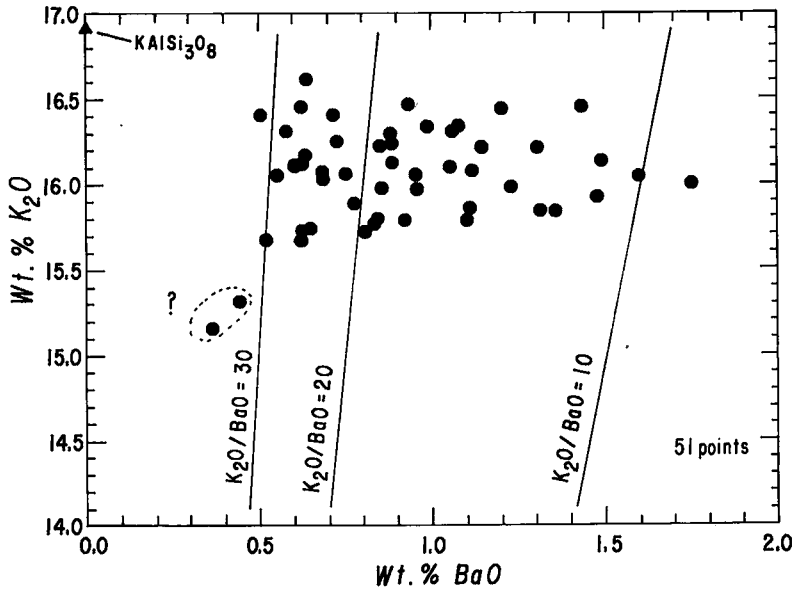


FIG. 2. Abundances of BaO and K₂O in exsolved alkali feldspar blebs in antiperthite from andesine anorthosite.

TABLE 1. REPRESENTATIVE COMPOSITIONS OF PLAGIOCLASE HOST IN ANTIPERTHITE

Wt. %	1.	2.	3.	4.	5.	6.	7.	8.	9.	10.	11.	12.	13.	14.	15.	16.	17.
SiO ₂	57.34	57.90	58.14	57.96	58.86	58.33	58.28	58.71	58.09	58.20	59.27	58.45	59.20	59.24	57.92	58.07	57.52
TiO ₂	0.04	0.03	0.00	0.00	0.03	0.03	0.03	0.01	0.00	0.03	0.02	0.02	0.05	0.01	0.05	0.03	0.00
Al ₂ O ₃	26.94	26.60	26.62	26.58	25.69	26.58	26.47	25.50	26.17	25.79	25.88	25.70	25.73	25.82	26.53	26.53	26.44
FeO	0.14	0.08	0.10	0.13	0.15	0.10	0.20	0.13	0.11	0.18	0.14	0.08	0.13	0.15	0.12	0.10	0.09
MgO	0.01	0.01	0.00	0.01	0.00	0.00	0.00	0.01	0.00	0.00	0.00	0.00	0.00	0.00	0.00	0.00	0.00
CaO	8.73	8.56	8.34	8.45	8.50	8.38	8.69	7.97	8.25	8.30	7.64	8.03	8.06	7.83	8.49	8.72	8.56
SrO	-	0.13	-	0.12	0.12	0.07	0.13	0.10	0.14	0.13	0.15	0.07	0.13	-	0.11	0.06	0.11
BaO	0.00	0.00	0.04	0.04	0.06	0.00	0.05	0.05	0.07	0.05	0.03	0.00	0.02	0.00	0.00	0.06	0.00
K ₂ O	0.41	0.39	0.34	0.39	0.39	0.36	0.32	0.43	0.21	0.27	0.30	0.19	0.31	0.44	0.33	0.39	0.37
Na ₂ O	6.28	6.46	6.77	6.81	6.40	6.69	6.49	6.84	6.86	6.76	7.14	6.97	6.91	6.85	6.58	6.62	6.43
Total	99.90	100.16	100.38	100.49	100.20	100.55	100.66	99.75	99.88	99.71	100.57	99.51	100.54	100.35	100.14	100.58	99.61

FORMULA PROPORTIONS BASED ON 8 OXYGEN ATOMS

Si	2.574	2.592	2.596	2.590	2.631	2.599	2.598	2.636	2.607	2.617	2.637	2.628	2.636	2.639	2.593	2.592	2.590
Ti	0.001	0.001	0.000	0.000	0.001	0.001	0.001	0.000	0.000	0.001	0.001	0.001	0.002	0.000	0.002	0.001	0.000
Al	1.425	1.403	1.401	1.400	1.353	1.396	1.391	1.350	1.381	1.367	1.357	1.362	1.350	1.356	1.400	1.396	1.404
Fe	0.005	0.003	0.004	0.005	0.006	0.004	0.007	0.005	0.004	0.007	0.005	0.003	0.005	0.006	0.005	0.004	0.007
Mg	0.001	0.001	0.000	0.001	0.000	0.000	0.000	0.001	0.000	0.000	0.000	0.000	0.000	0.000	0.000	0.000	0.000
Ca	0.420	0.411	0.399	0.405	0.407	0.400	0.415	0.383	0.397	0.400	0.364	0.387	0.384	0.374	0.407	0.417	0.413
Sr	-	0.003	-	0.003	0.003	0.002	0.003	0.003	0.004	0.003	0.004	0.002	0.003	-	0.003	0.002	0.003
Ba	0.000	0.000	0.001	0.001	0.001	0.000	0.001	0.001	0.001	0.001	0.001	0.000	0.000	0.000	0.000	0.001	0.000
K	0.023	0.022	0.021	0.022	0.022	0.021	0.018	0.025	0.012	0.015	0.017	0.011	0.018	0.025	0.019	0.022	0.021
Na	0.547	0.561	0.586	0.590	0.555	0.578	0.561	0.596	0.597	0.589	0.616	0.608	0.596	0.592	0.571	0.573	0.561
Σ	4.997	4.997	5.007	5.016	4.980	5.001	4.995	4.999	5.005	5.001	5.001	5.000	4.995	4.991	5.000	5.007	4.999

END-MEMBER PROPORTIONS

An	42.4	41.5	39.7	40.0	41.4	40.2	41.9	38.3	39.7	40.0	36.8	38.6	38.7	37.7	41.0	41.3	41.7
Ab	55.3	56.3	58.3	57.8	56.4	57.7	56.3	59.2	59.1	58.4	61.5	60.3	59.6	59.7	57.1	56.5	56.2
Or	2.3	2.2	2.1	2.2	2.3	2.1	1.8	2.5	1.2	1.5	1.7	1.1	1.8	2.5	1.9	2.2	2.1

[1] STU 24-19. [2] STU 24-20. [3] STU 22-22. [4] MLC P-368*. [5] MLC 20-4*. [6] STU 22-25. [7] MLC 19-2*. [8] STU 24-7. [9] MLC 20-3*. [10] CHV 80-76*. [11] STU 22-9. [12] STU 14-1A. [13] STU 22-11. [14] STU 24-18. [15] STU 22-23. [16] STU 25-7. [17] STU 24-21. - = not analyzed *samples from anorthositic dykes, Mont du Lac des Cygnes

TABLE 2. AVERAGE COMPOSITIONS OF POTASSIUM FELDSPAR BLEBS IN ANTIPERTHITHE

Wt. %	1.	2.	3.	4.	5.	6.	7.	8.	9.	10.	11.	12.	13.	14.	15.	16.	17.
SiO ₂	63.34	63.94	64.75	65.17	64.91	64.17	64.90	63.58	63.79	64.23	64.86	64.57	64.13	64.35	63.85	62.47	63.59
TiO ₂	0.00	0.01	0.01	0.00	0.05	0.02	0.05	0.00	0.00	0.05	0.03	0.03	0.05	0.00	0.01	0.05	0.00
Al ₂ O ₃	18.58	18.69	18.77	18.06	17.65	18.71	17.87	18.77	18.65	18.72	18.49	18.39	18.77	18.76	18.88	18.42	18.77
FeO	0.05	0.16	0.06	0.05	0.07	0.01	0.05	0.03	0.00	0.05	0.06	0.05	0.08	0.08	0.05	0.03	0.04
MgO	0.00	0.04	0.00	0.00	0.00	0.00	0.02	0.00	0.00	0.00	0.00	0.00	0.00	0.00	0.00	0.00	0.00
CaO	0.00	0.06	0.07	0.10	0.02	0.04	0.00	0.05	0.02	0.09	0.00	0.02	0.03	0.14	0.03	0.06	0.03
SrO	-	0.14	0.24	0.13	0.10	0.17	0.25	0.10	0.03	0.26	0.12	0.09	0.16	-	0.21	0.18	0.08
BaO	1.04	0.97	1.07	0.40	0.63	0.59	0.82	0.75	1.08	0.78	0.66	0.67	0.72	1.01	1.20	1.32	1.45
K ₂ O	16.03	16.20	16.33	15.24	16.18	16.10	15.77	16.30	15.99	16.18	15.72	16.43	16.44	15.89	16.16	16.45	15.96
Na ₂ O	0.33	0.25	0.24	0.28	0.31	0.33	0.29	0.22	0.28	0.34	0.32	0.24	0.19	0.20	0.24	0.18	0.27
Total	99.37	100.46	101.54	99.43	99.93	100.14	100.02	99.80	99.84	100.70	100.26	100.49	100.57	100.43	100.64	99.16	100.19

FORMULA PROPORTIONS BASED ON 8 OXYGEN ATOMS

Si	2.972	2.970	2.976	3.020	3.017	2.978	3.013	2.968	2.976	2.972	2.995	2.990	2.976	2.978	2.965	2.958	2.967
Ti	0.000	0.000	0.000	0.000	0.001	0.000	0.002	0.000	0.000	0.001	0.001	0.001	0.002	0.000	0.000	0.002	0.000
Al	1.028	1.024	1.018	0.987	0.967	1.023	0.978	1.033	1.026	1.021	1.006	1.004	1.025	1.024	1.033	1.028	1.032
Fe	0.002	0.006	0.002	0.002	0.003	0.000	0.002	0.001	0.000	0.001	0.002	0.002	0.003	0.003	0.002	0.001	0.002
Mg	0.000	0.003	0.000	0.000	0.000	0.000	0.001	0.000	0.000	0.000	0.000	0.000	0.000	0.000	0.000	0.000	0.000
Ca	0.000	0.002	0.003	0.005	0.001	0.002	0.000	0.002	0.001	0.005	0.000	0.001	0.001	0.007	0.001	0.002	0.001
Sr	-	0.006	0.006	0.004	0.003	0.005	0.007	0.003	0.001	0.007	0.003	0.002	0.005	-	0.006	0.005	0.002
Ba	0.020	0.018	0.019	0.008	0.011	0.015	0.014	0.014	0.020	0.014	0.012	0.012	0.013	0.018	0.022	0.024	0.027
K	0.960	0.960	0.958	0.901	0.960	0.953	0.934	0.971	0.952	0.955	0.926	0.971	0.971	0.938	0.957	0.994	0.950
Na	0.030	0.022	0.023	0.025	0.028	0.030	0.026	0.020	0.025	0.031	0.035	0.022	0.017	0.018	0.024	0.017	0.024
Σ	5.012	5.009	5.005	4.952	4.991	5.002	4.977	5.012	5.001	5.007	4.980	5.005	5.013	4.986	5.010	5.031	5.005

END-MEMBER PROPORTIONS

An	0.0	0.8	0.9	1.0	0.4	0.7	0.7	0.5	0.2	0.2	0.3	0.3	0.6	0.7	0.7	0.7	0.3
Ab	3.0	2.2	2.3	2.7	2.8	3.0	2.6	2.0	2.5	3.1	3.6	2.2	1.7	1.8	2.4	1.6	2.4
Or	95.0	95.2	94.9	95.5	95.7	95.3	95.1	96.1	95.2	94.4	94.9	96.3	96.4	95.6	94.8	95.4	94.6
Cn	2.0	1.8	1.9	0.8	1.1	1.1	1.5	1.4	2.0	1.4	1.2	1.2	1.3	1.8	2.2	2.3	2.7

[1] STU 24-19. [2] STU 24-20. [3] STU 22-22. [4] MLC P-368*. [5] MLC 20-4*. [6] STU 22-25. [7] MLC 19-2*. [8] STU 24-7. [9] MLC 20-3*. [10] CHV 80-76*. [11] STU 22-9. [12] STU 14-1A. [13] STU 22-11. [14] STU 24-18. [15] STU 22-23. [16] STU 25-7. [17] STU 24-21. - = not analyzed *samples from anorthositic dykes, Mont du Lac des Cygnes

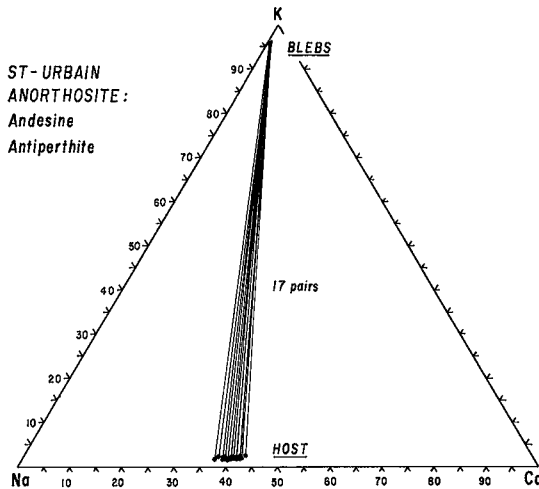


FIG. 3. A plot of atom % K-Na-Ca for antiperthite from andesine anorthosite.

K₂O (~ 0.2-0.4 wt.%) , FeO (~ 0.1-0.2 wt.%) and SrO (~ 0.1 wt.%) are typical of most compositions. Traces of Mg, Ba and Ti may also be present, but most values are below limits of detection (<0.05 wt.% each).

Compositions of blebs of exsolved alkali feldspar, representing the average of 3-5 analyses in each case, are listed in Table 2. Overall, the blebs show little variation in composition (ca. Or₉₅), being characterized by very high K, very low Na, and virtually no Ca. Similar K-rich compositions for blebs of exsolved alkali feldspar were reported by Anderson (1966) and Kay (1977).

Small amounts of Fe (~ 0.1 wt.% FeO) and Sr (~ 0.1-0.3 wt.% SrO) are present, but only traces of Mg and Ti occur. However, a noteworthy feature of the alkali feldspar is a large relative variation in Ba content (~ 0.4-1.6 wt.% BaO), such that K₂O/BaO ratios range from 10 to 30 (Fig. 2). Although this variation in Ba content may simply

reflect selective partitioning into potassium feldspar during exsolution, it is possible that changes in K/Ba ratio may ultimately provide important information on the course of differentiation of the andesine anorthosite (*cf.* Anderson 1966). Data on whole-rock samples are currently being gathered to evaluate this possibility.

Compositions of the plagioclase host and blebs of exsolved alkali feldspar are shown in Figure 3 in terms of atom % Ca, Na and K. Of particular note

is the low K content of the host, and the low Na and Ca contents of the blebs. Application of two-feldspar geothermometry (*e.g.*, Whitney & Stormer 1977) to these compositions yields temperatures of equilibration ranging from 310 to 380°C, averaging 345°C. It is highly unlikely, however, that these values represent the temperature at which exsolution was initiated, but probably reflect closure of K-Na exchange between host and bleb following a prolonged and complex thermal history.

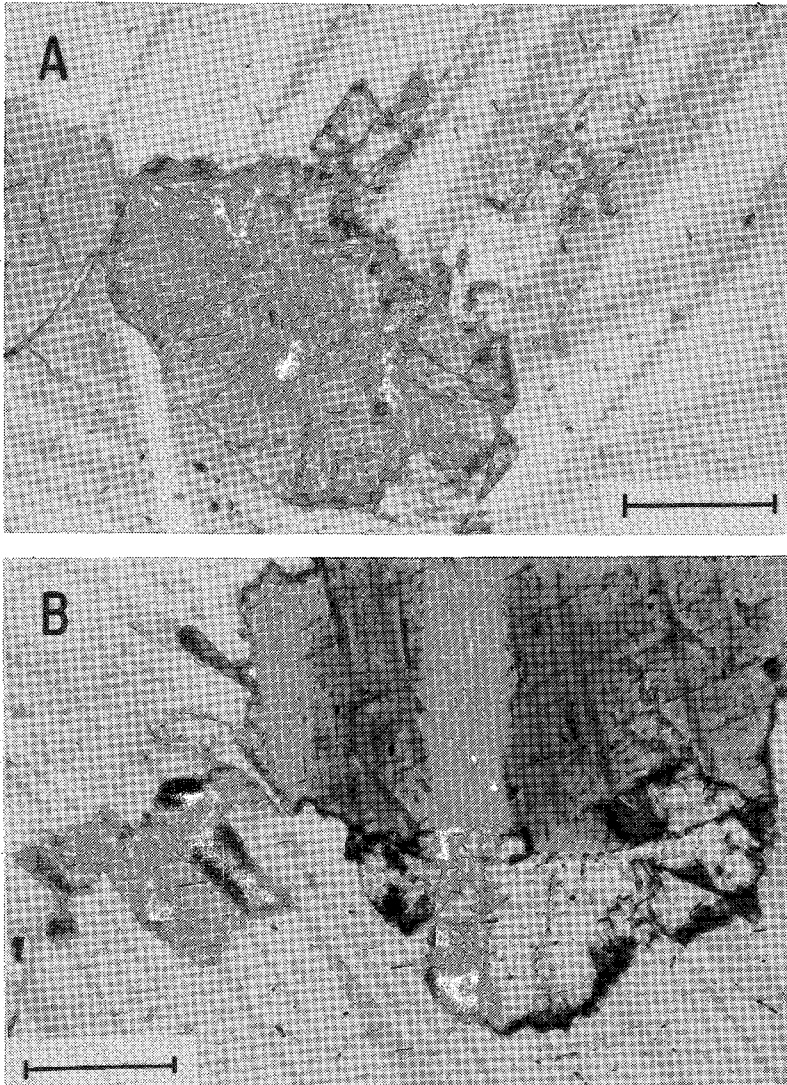


FIG. 4. A. Type-A myrmekite occurring as a subrounded aggregate between two plagioclase crystals in sample MLC 19-2; note elongate protrusions into top plagioclase grain (transmitted cross-polarized light; bar scale 500 μm). B. Type-A myrmekite extending from grain boundary into plagioclase in sample STU 24-7 (transmitted cross-polarized light; bar scale 500 μm).

MYRMEKITE

Methods of analysis and data presentation

Three varieties of "myrmekite" have been identified (termed types A, B and C, respectively), which are characterized in detail below. These have been analyzed for their bulk compositions and for the compositions of their constituent plagioclase. Myrmekite bulk-compositions were determined by microprobe analysis using an expanded electron-beam, where the spot diameter (30–50 μm) was adjusted to accommodate the size of the intergrowth in each case. At least three analyses were obtained on each sample.

The electron microanalysis of such multiphase aggregates is problematic, however, because standard matrix-correction procedures assume a homogeneous target as well as a general coincidence between the path lengths of the incident electron-beam and all generated X-rays. In the present case, these stipulations are not fulfilled, and an additional correction for an inhomogeneous target has been applied using the approach outlined by Albee *et al.* (1977). This method involves the calculation of a cation

norm from the initial analytical data, determination of correction factors for each element weighted against the abundance of that element in the normative minerals, recalculation of the bulk analysis, and reiteration. Since the myrmekites are "simple" quartz-feldspar intergrowths that lack a heavy absorber (*e.g.*, iron), the additional corrections are small, and of the same order of magnitude as the counting error associated with the analyses *per se* (~1–2% relative).

The myrmekite bulk-compositions have been recalculated to end-member proportions of An ($\text{CaAl}_2\text{Si}_2\text{O}_8$), Ab ($\text{NaAlSi}_3\text{O}_8$), Or (KAlSi_3O_8) and Qtz (as Si_4O_8), where $\text{Qtz} = 100 - \text{An} - \text{Ab} - \text{Or}$. The trace amounts of Mg, Fe, Ti, Ba and Sr were neglected in this calculation.

Volume % quartz (as SiO_2) in the myrmekites was calculated from their bulk compositions using the following expression:

$$\text{Vol. \% Qtz} = \frac{(4 \times \text{mole \% Si}_4\text{O}_8)(\bar{V}_{\text{Qtz}})}{(4 \times \text{mole \% Si}_4\text{O}_8)(\bar{V}_{\text{Qtz}}) + (\text{mole \% Fsp})(\bar{V}_{\text{Fsp}})}$$

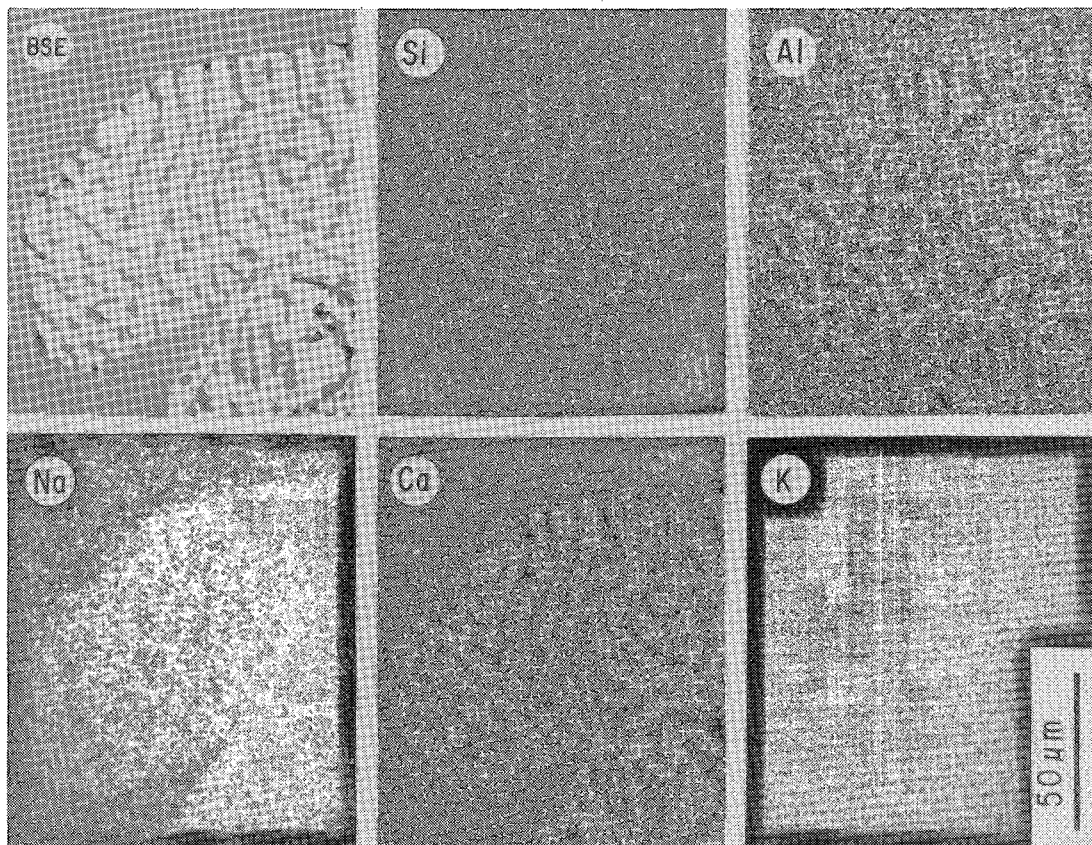


FIG. 5. Back-scattered electron (BSE) and X-ray images of a homogeneous type-A myrmekite from andesine anorthosite.

where $\bar{V}_{Fsp} = X_{An}\bar{V}_{An} + X_{Ab}\bar{V}_{Ab} + X_{Or}\bar{V}_{Or}$, and the factor of 4 reflects conversion of Si_4O_8 to SiO_2 . We have used the molar volume data of Robie *et al.* (1979) ($\bar{V}_{Qtz} = 22.69 \text{ cm}^3$; $\bar{V}_{An} = 100.79 \text{ cm}^3$; $\bar{V}_{Ab} = 100.07 \text{ cm}^3$; $\bar{V}_{Or} = 108.62 \text{ cm}^3$).

TYPE-A MYRMEKITE

Occurrence, form and distribution of elements

Type-A intergrowths comprise subrounded to subangular to plumose aggregates situated typically at plagioclase grain-boundaries (Fig. 4A), although a few appear to be enclosed entirely by plagioclase. These are the most common ones observed, and constitute up to ~ 1 volume % of some samples. Most are 100 to 500 μm in maximum dimension, although a few are as large as about 3 mm. The borders of the intergrowths are generally convex toward plagioclase, and in many cases the myrmekite penetrates far into one of the adjacent plagioclase grains,

which it seems to replace (Fig. 4B). Relict "islands" of the host plagioclase have been observed, which is consistent with a replacement origin.

Boundaries between the intergrowths and surrounding plagioclase are extremely sharp, being gently curved with some straight segments, although they may undulate on a μm scale. Observations in reflected light and use of back-scattered electron (BSE) imaging confirm the sharpness of the boundary and reveal the eutectic-like texture of the intergrowths. A portion of the most commonly observed variety of type-A myrmekite is illustrated in Figure 5. The BSE image shows the intergrowth to consist of a homogeneous bright-reflecting "matrix" (which is plagioclase) containing 20–30% uniformly distributed dark-reflecting 1–5- μm wide curvilinear "blebs" (which consist of quartz). This figure also shows the contrast in reflectivity between plagioclase in the host anorthosite and that in the intergrowth (which indicates a strong compositional difference), whereas the X-Ray images confirm that the myr-

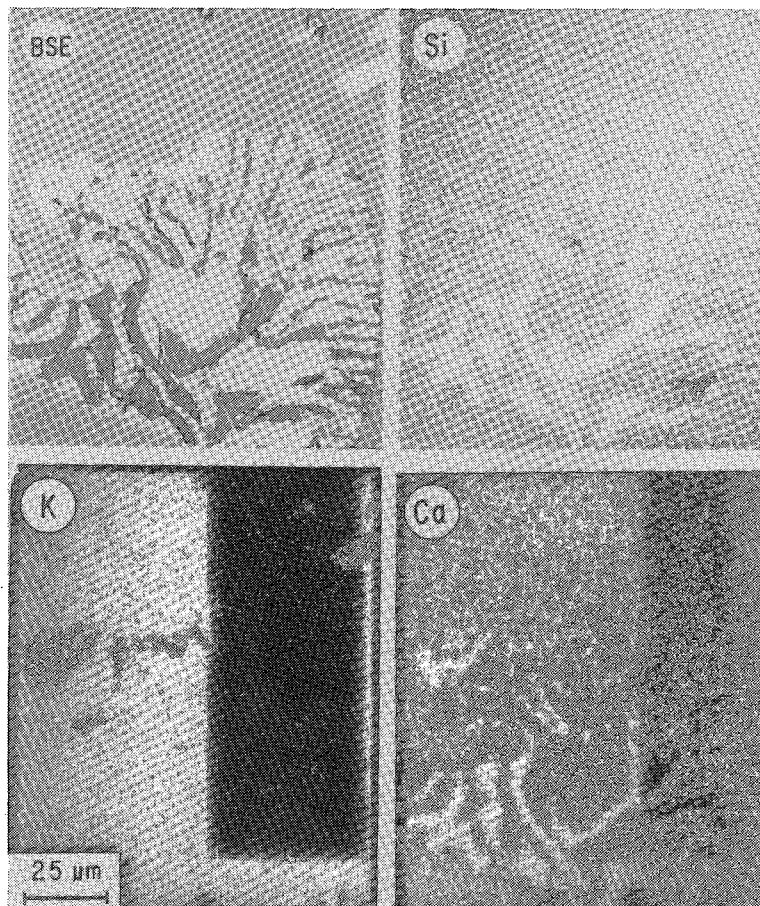


FIG. 6. BSE and X-ray images of a heterogeneous type-A myrmekite from andesine anorthosite.

mekite "matrix" is enriched in Ca and depleted in Na compared to the surrounding plagioclase, and that the intergrowth as a whole is devoid of K-rich material. The tendency of many quartz blebs to be oriented normal to the external interface can also be observed in Figure 5.

A second and less-common variety of type-A myrmekite is illustrated in Figure 6. It is characterized by a variation in the width of quartz blebs (producing a "cauliflower" texture) and the occurrence of minor K-rich areas at the innermost boundary with the host.

TABLE 3. BULK COMPOSITIONS OF TYPE-A MYRMEKITE

Wt. %	1.	2.	3.	4.	5.	6.	7.	8.	9.	10.
SiO ₂	60.38	58.15	57.25	58.39	59.93	60.54	59.56	59.24	58.61	59.88
TiO ₂	0.06	0.00	0.02	0.02	0.00	0.03	0.04	0.05	0.02	0.05
Al ₂ O ₃	25.22	26.90	27.29	26.34	25.03	25.59	25.61	24.74	27.08	25.25
FeO	0.16	0.05	0.06	0.22	0.06	0.07	0.12	0.17	0.13	0.18
MgO	0.03	0.00	0.01	0.00	0.02	0.00	0.01	0.00	0.00	0.00
CaO	11.79	13.16	13.78	13.31	13.22	13.06	13.29	13.10	13.44	13.35
SrO	0.13	0.10	-	0.06	0.07	0.07	0.10	-	0.06	0.07
BaO	0.02	0.00	0.02	0.03	0.02	0.01	0.02	0.04	0.01	0.01
K ₂ O	0.19	0.10	0.03	0.23	0.00	0.03	0.05	0.06	0.01	0.00
Na ₂ O	2.05	1.89	1.59	1.41	1.51	1.42	1.34	1.21	1.15	1.07
Total	100.03	100.35	100.05	100.01	99.86	100.82	100.15	98.60	100.50	99.86

FORMULA PROPORTIONS BASED ON 8 OXYGEN ATOMS

Si	2.677	2.585	2.556	2.605	2.665	2.663	2.644	2.667	2.593	2.661
Ti	0.002	0.000	0.001	0.001	0.000	0.001	0.001	0.002	0.001	0.002
Al	1.317	1.409	1.437	1.385	1.312	1.327	1.341	1.313	1.413	1.322
Fe	0.006	0.002	0.002	0.008	0.004	0.002	0.005	0.006	0.005	0.006
Mg	0.002	0.000	0.000	0.000	0.002	0.000	0.000	0.000	0.000	0.000
Ca	0.561	0.627	0.660	0.636	0.630	0.615	0.632	0.632	0.638	0.636
Sr	0.003	0.003	-	0.002	0.002	0.002	0.003	-	0.002	0.002
Ba	0.000	0.000	0.000	0.000	0.000	0.000	0.000	0.001	0.000	0.000
K	0.011	0.006	0.002	0.008	0.000	0.002	0.003	0.003	0.000	0.000
Na	0.176	0.163	0.137	0.122	0.130	0.121	0.115	0.105	0.099	0.093
Σ	4.753	4.795	4.795	4.767	4.745	4.733	4.744	4.729	4.751	4.722
Si+Al	3.994	3.994	3.993	3.990	3.977	3.990	3.985	3.980	4.006	3.983
Si/O*	0.335	0.323	0.320	0.326	0.333	0.333	0.331	0.333	0.324	0.333
X _{Ca} **	0.751	0.788	0.826	0.830	0.830	0.833	0.843	0.854	0.864	0.872
Vol. % Qtz†	23.3	18.5	18.5	21.6	22.2	24.2	23.1	24.0	24.3	25.1

END-MEMBER PROPORTIONS

An	56.1	63.0	66.0	63.6	63.0	61.5	63.2	63.2	63.8	63.6
Ab	17.6	16.3	13.7	12.2	13.0	12.1	11.5	10.5	9.9	9.3
Or	1.1	0.6	0.2	0.8	0.0	0.2	0.3	0.3	0.1	0.0
Qtz††	25.2	20.1	20.1	23.4	24.0	26.2	25.0	26.0	26.2	27.1

[1] STU 24-19 (4). [2] STU 24-20 (3). [3] STU 22-22 (5). [4] MLC P-368 (5).
 [5] MLC 20-4 (3). [6] STU 22-25 (3). [7] MLC 19-2 (10). [8] STU 24-7 (5).
 [9] MLC 20-3 (7). [10] CHV 80-76 (10).
 () = # of analyses averages
 - = not analyzed

* Si cations/oxygen associated with all cations

** X_{Ca} = Ca/(Ca+Na+K) atomic † as SiO₂ †† as □ Si₄O₈

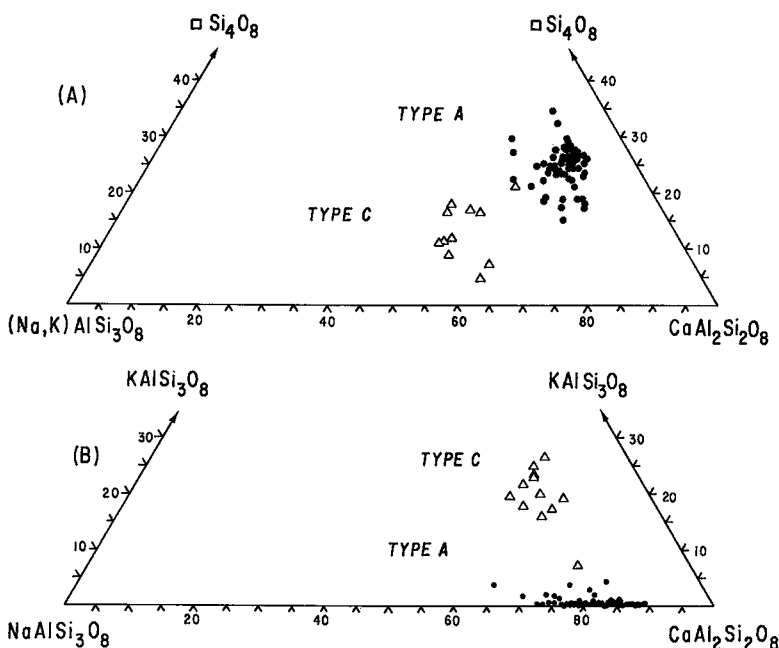


FIG. 7. Proportions of the feldspars and "quartz" (as $\square\text{Si}_4\text{O}_8$) in St-Urbain myrmekites, calculated from bulk compositions.

In transmitted plane-polarized light, the intergrowths are seen to consist of two colorless phases with differing indices of refraction, which indices are in turn different from those of the host plagioclase. Some intergrowths are brown and turbid, however, owing to the presence of Ca,Al-silicate alteration phases. In transmitted cross-polarized light, the plagioclase of the intergrowths is seen to consist of up to several grains that extinguish in different positions. It has not been possible to determine whether the quartz blebs represent optically continuous single grains or numerous smaller ones.

In general, the intergrowths are inclusion-free, although some contain oxide granules oriented parallel to (and possibly related to) those found in nearby plagioclase. In only one case was a K-feldspar bleb found within an intergrowth; this exception may represent the effect of a gently sloping grain boundary with the adjacent antiperthitic plagioclase.

Bulk compositions

Bulk compositions of type-A myrmekite from 10 samples are listed in Table 3, where they are arranged

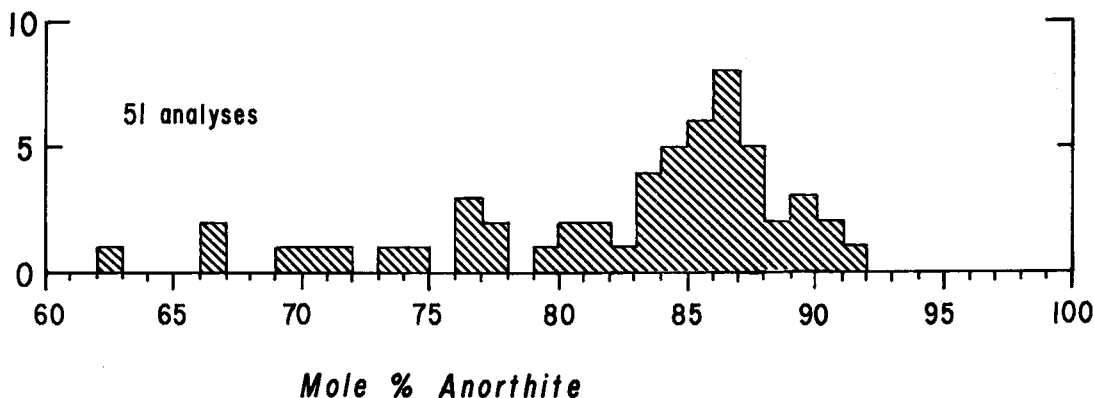


FIG. 8. Histogram of plagioclase compositions in type-A myrmekite.

in order of increasing $X_{Ca} [= Ca/(Ca + Na + K)]$. [Analyses were also obtained on myrmekites in 6 other samples, for which additional mineral-chemical data are presented in Tables 1, 2, 4 and 7, but these results are not reported because they are considered unreliable owing to low analytical totals (85–95 wt. %) caused by combinations of alteration and poor polishing. Nevertheless, the relative oxide abundances in these other analyses are in good agreement with the compositions that are listed in Table 3.] These compositions are characterized by high contents of Ca, Al and Si, relatively low Na, and virtually no K. Values for Mg, Fe and Ti are also very low, which precludes the presence of mafic silicates or oxides from the intergrowths. Quartz contents calculated from these average bulk-compositions range

from 20 to 27 mole % $\square Si_4O_8$. This corresponds to a range of calculated volume % quartz (as SiO_2) from 18.5 to 25.1%, which is entirely compatible with visual estimates.

Other noteworthy features of these analyses include variable X_{Ca} (corresponding to a range of average plagioclase compositions from An_{75} to An_{87}), relatively constant formula-proportions for (Si + Al) at 4.0 (a value expected for a quartz-feldspar intergrowth), and relatively constant Si/O at 0.333 (an unanticipated result, which is discussed in detail later). Further inspection of the data reveals a very slight excess in Al [*i.e.*, $Al > (2Ca + Na + K)$], which most likely reflects analytical error rather than anything significant about the bulk compositions.

In order to show that averaging has not biased our

TABLE 4. COMPOSITIONS OF PLAGIOCLASE IN TYPE-A MYRMEKITE[†]

Wt. %	1.	2.	3.	4.	5.	6.	7.	8.	9.	10.	11.	12.	13.	15.	17.
SiO ₂	46.33	46.74	46.21	47.40	45.25	46.65	46.95	45.95	46.70	47.81	52.30	46.46	47.23	51.55	51.01
TiO ₂	0.00	0.00	0.00	0.00	0.00	0.00	0.00	0.06	0.00	0.00	0.00	0.04	0.02	0.00	0.05
Al ₂ O ₃	34.29	34.23	34.70	33.54	34.37	34.58	33.96	34.24	33.91	33.08	30.61	34.33	33.77	31.76	30.76
FeO	0.12	0.12	0.00	0.12	0.13	0.08	0.14	0.08	0.11	0.11	0.21	0.13	0.20	0.09	0.12
MgO	0.00	0.00	0.02	0.00	0.00	0.00	0.02	0.00	0.00	0.00	0.06	0.00	0.00	0.00	0.00
CaO	17.04	17.25	17.75	17.73	17.50	17.32	17.42	17.08	16.91	16.34	12.24	16.99	17.15	14.07	13.41
SrO	0.17	0.27	-	0.15	0.18	0.11	0.13	0.09	0.13	0.11	0.10	0.21	0.14	0.15	0.10
BaO	0.00	0.00	0.00	0.02	0.00	0.04	0.00	0.00	0.00	0.01	0.00	0.04	0.00	0.02	0.00
K ₂ O	0.05	0.05	0.00	0.04	0.04	0.03	0.06	0.07	0.06	0.05	0.16	0.04	0.07	0.28	0.15
Na ₂ O	1.58	1.67	1.60	0.94	1.39	1.65	1.64	1.56	1.80	2.01	3.98	1.70	1.48	3.20	3.65
Total	99.57	100.33	100.28	99.93	98.86	100.46	100.29	99.12	99.62	99.51	99.65	99.96	100.07	101.12	99.25

FORMULA PROPORTIONS BASED ON 8 OXYGEN ATOMS

Si	2.139	2.144	2.120	2.176	2.110	2.136	2.153	2.131	2.154	2.201	2.376	2.138	2.168	2.320	2.337
Ti	0.000	0.000	0.000	0.000	0.000	0.000	0.000	0.002	0.000	0.000	0.000	0.001	0.001	0.000	0.002
Al	1.865	1.851	1.876	1.815	1.889	1.866	1.836	1.872	1.844	1.795	1.639	1.862	1.827	1.684	1.661
Fe	0.005	0.005	0.000	0.005	0.005	0.003	0.005	0.003	0.004	0.004	0.008	0.005	0.008	0.003	0.005
Mg	0.000	0.000	0.001	0.000	0.000	0.000	0.001	0.000	0.000	0.000	0.004	0.000	0.000	0.000	0.000
Ca	0.843	0.848	0.873	0.872	0.874	0.850	0.856	0.849	0.836	0.806	0.596	0.838	0.844	0.678	0.658
Sr	0.005	0.007	-	0.004	0.005	0.003	0.004	0.002	0.003	0.003	0.003	0.006	0.004	0.004	0.003
Ba	0.000	0.000	0.000	0.000	0.000	0.001	0.000	0.000	0.000	0.000	0.000	0.001	0.000	0.000	0.000
K	0.003	0.003	0.000	0.002	0.002	0.002	0.003	0.004	0.003	0.003	0.009	0.002	0.004	0.016	0.009
Na	0.142	0.148	0.142	0.084	0.125	0.147	0.146	0.141	0.161	0.179	0.350	0.152	0.132	0.280	0.325
Σ	5.000	5.006	5.012	4.958	5.010	5.006	5.004	5.003	5.006	4.992	4.984	5.006	4.986	4.986	4.998

END-MEMBER PROPORTIONS

An	85.4	85.0	86.0	91.1	87.4	85.1	85.2	85.4	83.6	81.6	62.5	84.6	86.2	69.7	66.4
An	14.3	14.7	14.0	8.7	12.4	14.6	14.5	14.2	16.1	18.1	36.5	15.2	13.4	28.6	32.7
Or	0.3	0.3	0.0	0.2	0.2	0.2	0.3	0.4	0.3	0.3	0.9	0.2	0.4	1.6	0.9

[1] STU 24-19. [2] STU 24-20. [3] STU 22-22. [4] MLC P-368*. [5] MLC 20-4*. [6] STU 22-25. [7] MLC 19-2*. [8] STU 24-7. [9] MLC 20-3*. [10] CHV 80-76*. [11] STU 22-9. [12] STU 14-1A. [13] STU 22-11. [15] STU 22-23. [17] STU 24-21. * samples of anorthosite dykes from Mont du Lac des Cygnes

[†] analysis #'s keyed to data in Tables 1 and 2

- = not analyzed

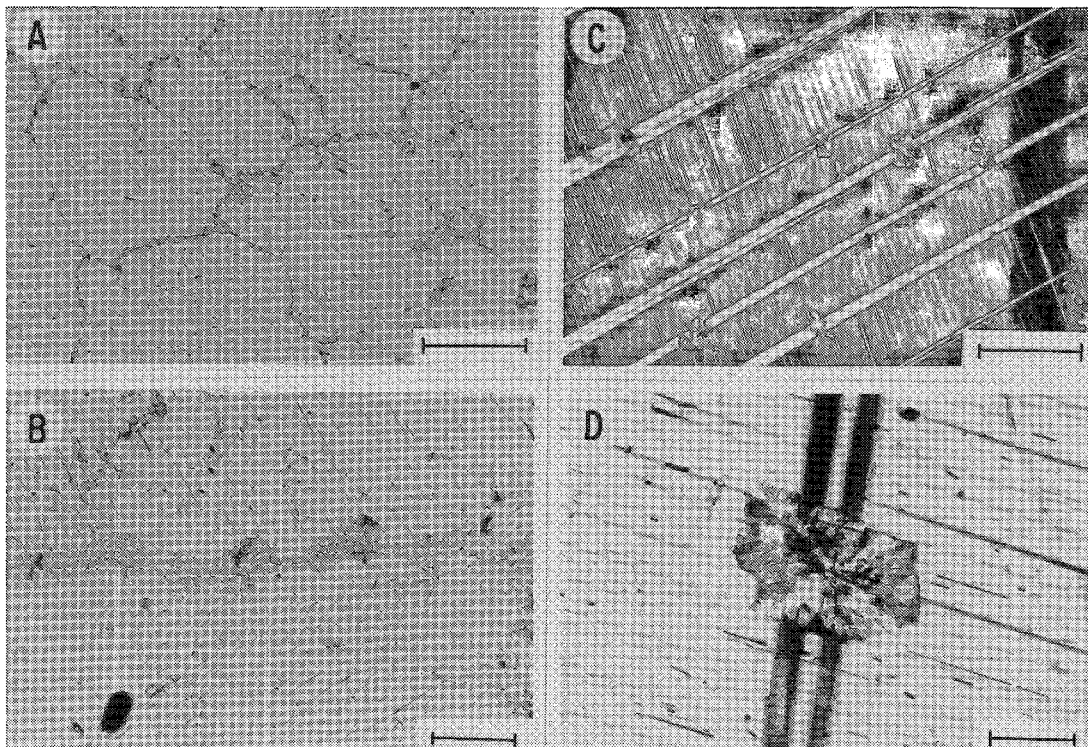


FIG. 9. A. Type-B myrmekite appearing as a dark film decorating plagioclase grain-boundaries in sample MLC 20-3 (transmitted plane-polarized light; bar scale 1 mm). B. Close-up view of type-B myrmekite shown in Figure 9A (transmitted plane-polarized light; bar scale 100 μm). C. Type-C myrmekite forming blocky "inclusions" in plagioclase megacryst in sample MLC 19-2 (transmitted cross-polarized light; bar scale 1 mm). D. Close-up view of type-C myrmekite shown in Figure 9C (transmitted cross-polarized light; bar scale 100 μm).

presentation, we have plotted in Figure 7A the relative proportions of Qtz-An-(Ab + Or) for the 59 individual bulk-compositions; the same data are illustrated on Figure 7B, plotted in terms of relative proportions An-Ab-Or. In both cases, the clustering of the data points is evident, indicating that the averages provide a useful representation of the entire data-set.

Compositions of constituent plagioclase

A representative composition of plagioclase from each of the ten examples of myrmekite described above, and for five others on which useful bulk-analyses could not be obtained, are listed in Table 4. These mineral analyses complement and extend the bulk analyses, and confirm that plagioclase in the intergrowths is universally more calcic than that in the host anorthosite (*cf.* Table 1).

A histogram of all analyzed plagioclase in type-A myrmekite is illustrated in Figure 8. Although the total range of measured compositions is An₆₀ to An₉₂, the majority fall within a more restricted

range, from An₈₀ to An₉₀. This is not an artifact of sampling, but a realistic representation of the actual distribution of plagioclase compositions. In fact, some of the more sodic compositions may not be part of a "new" myrmekite feldspar, but may be modified "relics" of the original host plagioclase. Additional information on this point is presented in a subsequent section.

TYPE-B MYRMEKITE

Type-B intergrowths comprise 10- to 100- μm wide semicontinuous "films" that decorate plagioclase grain-boundaries. These locally widen and appear to grade into type-A intergrowths, and their textural (and chemical) characteristics are largely indistinguishable from those outlined above. Type-B intergrowths seem more susceptible to alteration than those of type A, and in several samples, plagioclase grain-boundaries are accentuated by this brown material. Photomicrographs of typical type-B intergrowths are illustrated in Figures 9A and 9B, and

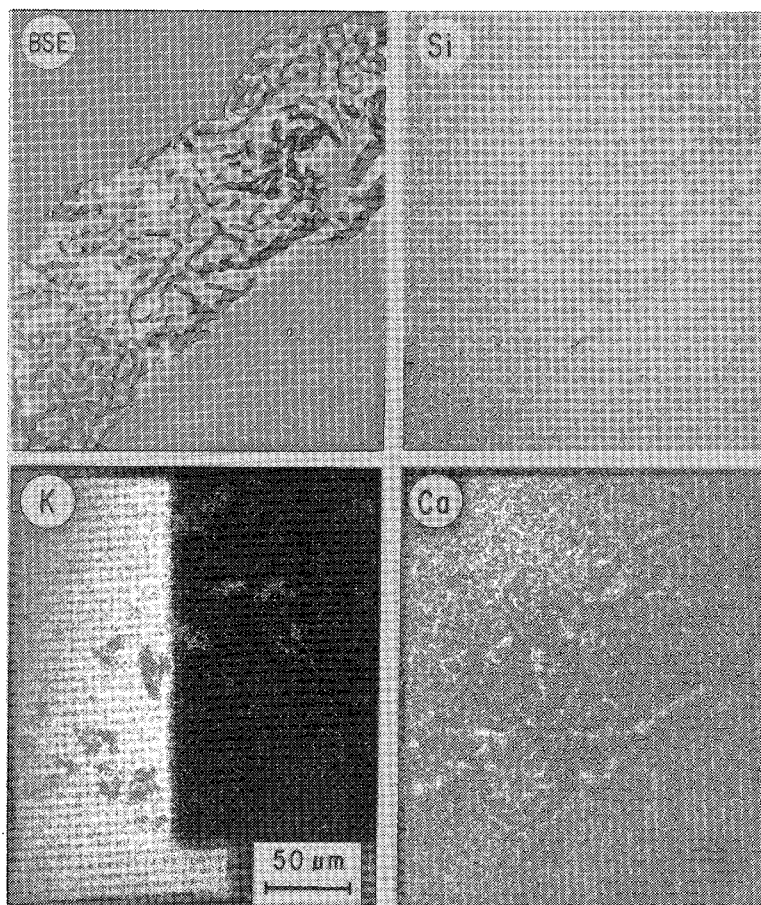


FIG. 10. BSE and X-ray images of a type-B myrmekite from andesine anorthosite.

combined BSE and X-ray images are shown in Figure 10. Because of the obvious similarity between type-A and type-B intergrowths, detailed chemical data are not presented for the latter.

TYPE-C MYRMEKITE

Occurrence and texture

Type-C intergrowths comprise aggregates up to 200 μm across that occur as rectangular "inclusions" in plagioclase megacrysts, but as yet have been identified in only one sample (MLC 19-2), where approximately 2 dozen were found. However, these may not be inclusions at all, but may actually be cross-sections of "tubes" penetrating into the megacrysts from their margins. A systematic study of megacrysts will be required to assess the appearance of these objects in three dimensions.

As shown in Figure 9C, the intergrowths are found typically at albite twin lamellae, but both the albite and pericline twins pass unimpeded through them. Each intergrowth shows a characteristic "bow-tie" structure (Fig. 9D), which in many cases contains a kernel of an Fe-Ti oxide granule. Many are altered to a brown turbid material that has a composition similar to the zeolite mineral phillipsite (Table 5, #4).

BSE and X-ray imaging (Fig. 11) confirms that these intergrowths are enriched in Ca and depleted in Na compared to the enclosing plagioclase megacryst. Moreover, they contain K-rich regions, and seem to be surrounded in part by grains of K-feldspar whose size, shape and chemical composition (Table 5, #3) are not unlike the exsolved blebs found throughout the megacrysts. It is unclear whether these K-feldspar "rinds" indicate that the myrmekite acted as a nucleation site for their later growth, or whether the myrmekites formed later and "pushed aside" the K-feldspar as they grew.

Composition

The average composition of a type-C intergrowth from sample MLC 19-2 is listed in Table 5 (#1). Like the type-A myrmekites discussed above, this variety is also characterized by high Ca, Al and Si, and relatively low Na. However, it is distinguished from all other examples by a high K-content. In terms of relative proportions of quartz and feldspar (Fig. 7A), the individual compositions of these intergrowths are shifted toward the (Ab + Or) corner compared to data for type A. However, this shift appears to be caused principally by a higher Or-content, since the An/(An + Ab) of the individual bulk-compositions are within the range observed for type-A myrmekites (Fig. 9B). In addition, plagioclase within the type-C myrmekite has a composition An₈₂ (Table 5, #3), also similar to values for type A (*cf.* Table 4, Fig. 8). Consequently, it is unclear whether the type-C intergrowth represents a type-A myrmekite that somehow incorporated K-feldspar (from exsolved blebs?) during its formation, or represents a fundamentally different entity. Further consideration of type-C myrmekite is best deferred until additional examples are identified.

MISCELLANEOUS INTERGROWTHS

The use of BSE imaging has facilitated greatly the recognition and characterization of a variety of other types of intergrowths. Three examples are discussed below that share some textural and chemical characteristics with the myrmekites. In addition, data are presented on some rare occurrences of what appear to be secondary alteration-phases that introduce further complications into a full understanding and interpretation of the history of the anorthosite massif. The main purpose for presenting information of this type is to call attention to the extraordinary level of unanticipated small-scale complexity that has been observed. It is difficult to evaluate the abundance of these other intergrowths, but our impressions at this time suggest that they are quantitatively insignificant.

The first variety comprises very fine-grained, porous-looking quartz-plagioclase aggregates along plagioclase grain-boundaries of the host anorthosite (Fig. 12A). Plagioclase in these intergrowths is complex, and consists of a rounded core (with a composition like that of the host anorthosite, *i.e.*, An₄₀) surrounded by a more calcic rim (Table 6, #9) which, in a few cases, penetrates the core along what appear to be cleavage planes (Fig. 12B). These textures indicate a replacement origin for the intergrowths, and the association of quartz + calcic plagioclase suggests some type of link to the myrmekites.

The second variety (Fig. 12C,D) forms very fine-grained pale-green quartz-rich vermicular inter-

growths with a texture like that of myrmekite. However, a bulk analysis (Table 6, #11) indicates a mineralogy consisting predominantly of quartz + albite + chlorite. Detailed examination also reveals the presence of rare more calcic plagioclase with a composition near An₅₀ (Table 6, #10). The origin of this type of intergrowth is unknown, although the presence again of quartz + calcic plagioclase permits some type of relationship to myrmekite.

The third intergrowth (Fig. 13), which is also found at plagioclase grain-boundaries of the host anorthosite, consists of quartz and feldspar with a remarkable diversity of compositions. These are summarized in Figure 14, and representative compositions are listed in Table 6 (#1-5; the locations of the analyzed spots are shown in Fig. 13).

The most prominent features found here are 10- to 25- μ m wide "veinlets" of albite (compare Na and Ca X-ray maps) intergrown with quartz, which separate grains of matrix plagioclase and enclose subangular plagioclase that is reversely zoned in a

TABLE 5. COMPOSITIONS FROM A TYPE-C MYRMEKITE IN SAMPLE MLC 19-2

Wt. %	1.	2.	3.	4.
SiO ₂	57.67	47.91	64.16	48.15
TiO ₂	0.05	0.00	0.02	0.02
Al ₂ O ₃	25.74	33.69	18.38	25.03
FeO	0.12	0.14	0.12	0.04
MgO	0.03	0.00	0.00	0.00
CaO	11.25	16.79	0.13	11.96
SrO	0.16	0.20	0.20	0.02
BaO	0.02	0.00	0.79	0.00
K ₂ O	3.03	0.06	15.79	0.14
Na ₂ O	1.65	1.98	0.24	1.11
Total	99.71	100.69	99.73	86.47
FORMULA PROPORTIONS*				
Si	2.610	2.185	2.989	9.960
Ti	0.002	0.000	0.001	0.004
Al	1.374	1.807	1.009	6.113
Fe	0.004	0.005	0.001	0.008
Mg	0.002	0.000	0.000	0.000
Ca	0.546	0.820	0.006	2.655
Sr	0.004	0.005	0.005	0.002
Ba	0.000	0.000	0.014	0.000
K	0.144	0.003	0.938	0.038
Na	0.175	0.175	0.022	0.444
Σ	4.861	5.001	4.986	19.224
END-MEMBERS PROPORTIONS				
An	55.0	82.2	1.1	-
Ab	14.4	17.5	2.2	-
Or	17.5	0.3	95.2	-
Qtz [†]	13.1	-	-	-
Cn	-	-	1.4	-

[1] Bulk composition (avg. of 11 analyses).
 [2] Plagioclase. [3] Alkali feldspar.
 [4] Brown alteration material whose formula, (Na,K)_{0.5}Ca_{2.5}Al₆Si₁₀O₁₆·6H₂O, is close to phillipsite (avg. of 3 analyses).

* #1-3 based on 8 oxygen atoms; #4 based on 32 oxygen atoms † as □Si₄O₈

TABLE 6. COMPOSITIONS OF FELDSPARS, PREHNITE, AND BULK COMPOSITIONS FROM MISCELLANEOUS INTERGROWTHS

Sample	24-21	24-21	24-21	24-21	24-21	24-18	24-18	22-25	24-19	22-11	22-11
Wt. %	1.	2.	3.	4.	5.	6.	7.	8.	9.	10.	11.
SiO ₂	53.24	67.46	56.32	57.98	63.68	64.55	42.83	45.03	55.21	55.69	83.89
TiO ₂	0.03	0.03	0.06	0.02	0.06	0.17	0.22	0.09	0.00	0.02	0.00
Al ₂ O ₃	29.14	20.05	27.27	24.08	19.27	21.04	22.98	23.10	28.17	28.72	8.53
FeO	0.18	0.02	0.09	0.22	0.21	0.00	0.45	1.30	0.06	0.18	1.11
MgO	0.00	0.00	0.00	0.29	0.29	0.11	0.00	0.12	0.00	0.03	1.48
CaO	11.87	0.58	9.69	3.34	0.19	1.09	25.92	23.19	9.81	10.51	0.32
SrO	0.12	0.16	0.03	0.19	0.10	0.17	0.04	0.00	0.25	0.23	0.06
BaO	0.00	0.00	0.22	0.15	0.24	0.00	0.00	0.01	0.00	0.00	0.02
K ₂ O	0.25	0.06	0.27	10.10	13.52	0.54	0.01	0.25	0.15	0.23	0.25
Na ₂ O	4.57	11.17	5.84	1.73	1.07	10.41	0.13	1.17	5.62	5.29	3.15
Total	99.41	99.54	99.78	98.09	98.64	98.09	92.58	94.26	99.26	100.89	98.81

FORMULA PROPORTIONS*											
Si	2.425	2.965	2.540	2.712	2.959	2.896	3.041	3.126	2.503	2.488	8.078
Ti	0.001	0.001	0.002	0.001	0.002	0.000	0.011	0.005	0.000	0.002	0.000
Al	1.565	1.039	1.450	1.327	1.056	1.113	1.923	1.890	1.505	1.512	0.967
Fe	0.007	0.001	0.004	0.008	0.008	0.006	0.027	0.075	0.002	0.007	0.089
Mg	0.000	0.000	0.000	0.020	0.020	0.007	0.000	0.000	0.013	0.002	0.212
Ca	0.580	0.027	0.468	0.168	0.010	0.053	1.972	1.725	0.477	0.503	0.033
Sr	0.003	0.004	0.006	0.005	0.003	0.004	0.002	0.000	0.007	0.006	0.003
Ba	0.000	0.000	0.000	0.003	0.004	0.000	0.000	0.000	0.000	0.000	0.000
K	0.015	0.003	0.016	0.603	0.802	0.031	0.001	0.022	0.008	0.013	0.030
Na	0.404	0.952	0.511	0.157	0.097	0.905	0.018	0.158	0.494	0.459	0.587
Σ	5.000	4.992	4.996	5.003	4.960	5.015	6.995	7.014	4.995	4.990	36.504

END-MEMBER PROPORTIONS											
An	58.2	3.1	47.4	18.4	1.4	5.7	-	-	49.0	51.9	-
Ab	40.3	96.6	51.0	16.8	10.6	91.1	-	-	50.1	46.8	-
Or	1.4	0.3	1.6	64.4	87.6	3.1	-	-	0.8	1.3	-

[1] Resorbed (?) plagioclase enclosed in albite; compositions in this association range from An₄₉₋₅₀. [2] Replacement albite; compositions range from An₂₋₅. [3] Reversely zoned plagioclase near albite veinlet; compositions range from An₄₀₋₄₇. [4] Bulk composition of globular two-feldspar intergrowth (composition considered approximate). [5] Bladed secondary albite. [6] Spongy secondary albite. [7] Bladed secondary prehnite. [8] Secondary prehnite. [9] Replacement rim on An₄₀ plagioclase. [10] Relict plagioclase from quartz-rich vermicular intergrowth. [11] Bulk composition of quartz-rich intergrowth.

* #1-6, 9 & 10 normalized to 8 oxygen atoms; #7 & 8 normalized to 11 oxygen atoms; #11 normalized to 10 cations for convenience (summation represents calculated total positive charge).

radial fashion from An₅₀ (core) to An₆₀ (rim). The plagioclase of the surrounding host anorthosite is reversely zoned in the vicinity of the intergrowth as well; the wavy arrows in Figure 13 indicate the direction of increasing An-content, which changes from An₄₀ to An₄₈ adjacent to the albite. Also observed in this intergrowth are globular two-feldspar intergrowths whose locations are indicated by the K-rich areas (see Fig. 13). The approximate compositions of this object and of its constituent K-feldspar are listed in Table 6 (#4, 5); a low Ba-content distinguishes this K-feldspar from the antiperthite blebs (cf. Table 2, Fig. 2).

It appears that this intergrowth as a whole signifies some type of late "albitization" event; whether

reverse zoning in the plagioclase developed at this time is unclear. It is possible that the albite was superimposed on features established at grain boundaries during an earlier episode of myrmekite formation; plagioclase in type-A myrmekite from this sample is more sodic than in most others (Table 4, #17), perhaps indicating late modification.

Albite also occurs in a few other samples, where it has a "spongy" texture, and may be intergrown with bladed prehnite. Compositions of these phases from sample STU 24-18 are listed in Table 6 (#6, 7). This sample has a mottled, bleached appearance, suggesting some type of secondary alteration.

Prehnite has also been identified in other samples (without albite), where it occurs as coarse fracture-

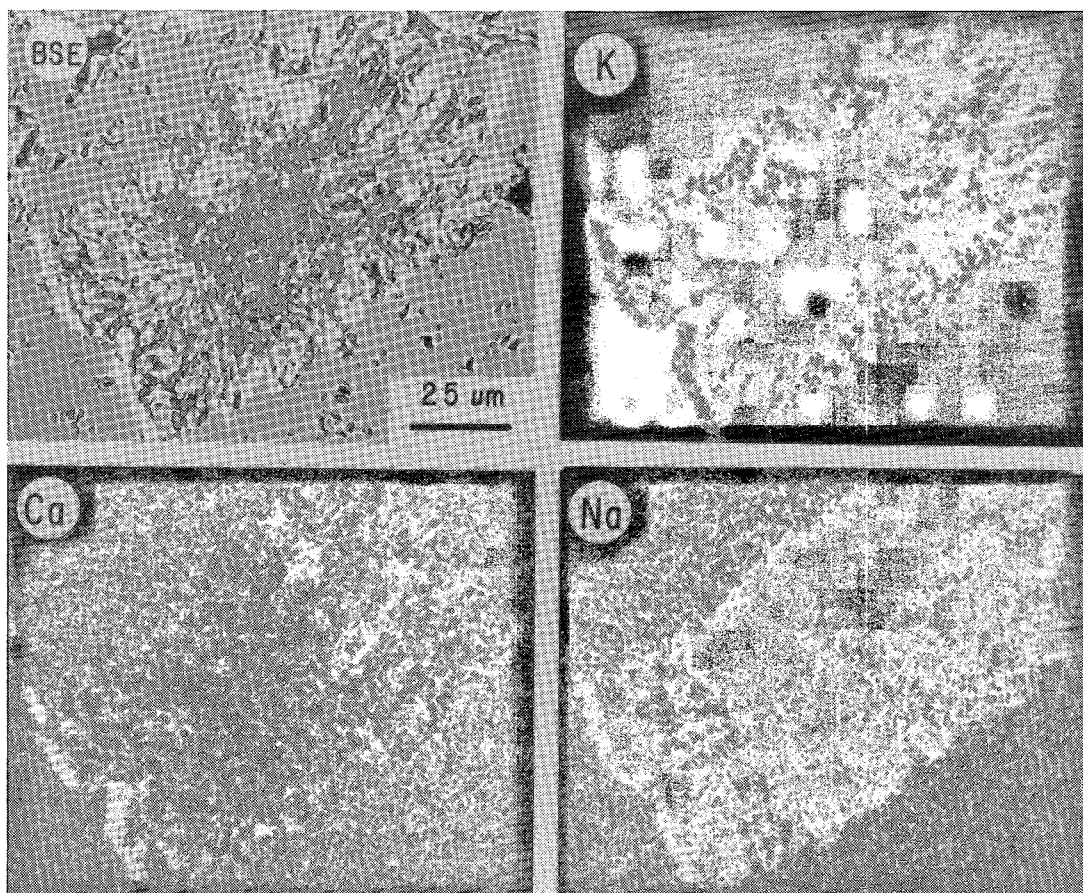


FIG. 11. BSE and X-ray images of a type-C myrmekite; note abundant K-rich areas, in contrast to myrmekites of types A and B.

filling material or as tiny (5–25 μm) grains that replace plagioclase. A composition of the latter variety from sample STU 22–25 appears in Table 6 (#8).

DISCUSSION: OVERVIEW

An extensive literature exists on myrmekite, which has been reviewed recently by Phillips (1974, 1980), Shul-diner (1972), and Smith (1974). Some authors use the term myrmekite in a descriptive, nongenetic sense applied to vermicular intergrowths of plagioclase feldspar + quartz, and note that such intergrowths are found only rarely in mafic igneous rocks, but are common accessory constituents of many granitic plutonic rocks and quartzofeldspathic gneisses. Phillips (1974), however, restricts the definition of myrmekite to intergrowths of *sodic* plagioclase + quartz that separate potassium feldspar from plagioclase (which is typically more calcic than that found in the myrmekite). Because the St-Urbain myrmekites consist of *calcic* plagioclase

+ quartz and lack the associated alkali feldspar, they appear to be fundamentally different from most occurrences discussed by previous investigators. These differences must be taken into account when applying earlier ideas on myrmekite genesis to St-Urbain.

The anorthosite samples reported on in this paper were collected from widely separated localities within the St-Urbain massif (Fig. 1). Nevertheless, the data show very similar compositions for the host antiperthite (Fig. 3) and only a limited range in myrmekite compositions (Table 3). It seems reasonable to suggest that a similar process has operated to produce these myrmekites, and that the widespread occurrence of such intergrowths at St-Urbain has an important bearing on the details of crystallization of this anorthositic pluton. However, it is important at this juncture to inquire as to whether this occurrence of calcic myrmekite is unique to St-Urbain, or whether the results obtained here have more general applicability.

MYRMEKITES (?) IN OTHER ANORTHOSITIC ROCKS

The literature on anorthosites contains several descriptions of features that broadly resemble the myrmekite found at St-Urbain. For example, Pavlov & Karskii (1949) described and illustrated myrmekite in labradorite anorthosite from an unspecified locality in the Soviet Union that consists of intergrown An_{80} + quartz. Morin (1956) noted the presence of "myrmekitic structures" interstitial to plagioclase in andesine anorthosite from the Labrieville area, Quebec, but unfortunately provided no details of this occurrence. Emslie (1980, Fig. 27C) illustrated a vermicular intergrowth in anorthosite from the Harp Lake Complex, Labrador, which consists of calcic plagioclase + K-rich alkali feldspar; perhaps further study will reveal quartz in addition. Guanghong (1982) described anorthosite from the

Damiao massif, People's Republic of China, and illustrated andesine antiperthite in which grain boundaries are decorated with fine-grained bulbous aggregates that appear similar to those shown here (*cf.* Fig. 4, 9A); although he did not draw attention to these objects, we suspect that they are myrmekite. Carstens (1967, Figs. 9–12) illustrated curious vermicular intergrowths in anorthosite from Egersund, Norway, which bear an uncanny resemblance to the St-Urbain myrmekites. He indicated that the Egersund intergrowths consist of plagioclase + alkali feldspar, representing an antiperthite formed by a "discontinuous precipitation" mechanism. However, neither optical nor chemical data were presented; these occurrences should be examined in detail as our own cursory study on samples of Egersund anorthosite indicate that these intergrowths are myrmekite. In addition, we have observed myrmekite in anor-

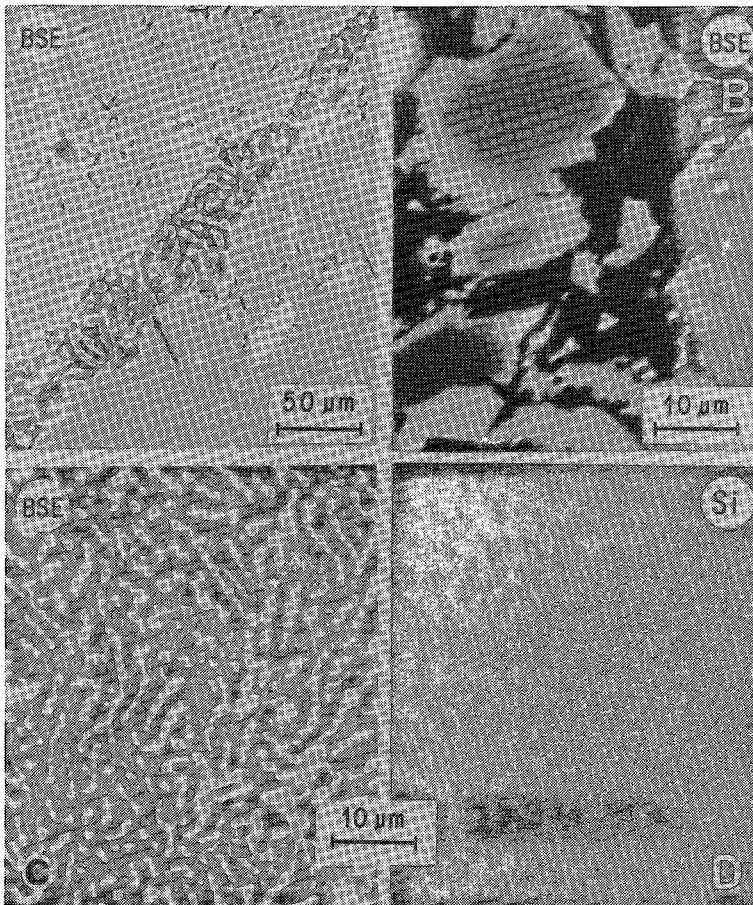


FIG. 12. A. BSE image of quartz-rich grain-boundary intergrowth. B. BSE image of area near arrow in Figure 12A, showing "mantled" feldspar in which An_{50} surrounds An_{40} . C, D. BSE and Si X-ray images of quartz-chlorite-albite intergrowth.

thosite from the Lac Allard massif, Quebec and from the River Valley massif, Ontario.

Myrmekite also occurs in layered mafic intrusive complexes. Salpas *et al.* (1983) noted its development in anorthosites from the Middle Banded Zone of the Stillwater Complex. Wager & Brown (1968) and Von Gruenewaldt (1979) described and illustrated myrmekite from the Bushveld Complex and observed that it is associated with reversely zoned plagioclase. Preliminary results of our own study of myrmekite from the Bushveld Complex indicate that there are textural and chemical similarities between these intergrowths and the calcic myrmekite from St-Urbain.

In summary, although the literature does not contain a large body of corroborative observations, there are a sufficient number of intriguing intergrowths reported in other anorthositic rocks to warrant further investigation of this problem. It is possible that calcic myrmekite has been overlooked frequently,

and will emerge as a common feature of massif anorthosites and other plagioclase-rich igneous cumulates.

ORIGIN OF CALCIC MYRMEKITE

The origin of myrmekite has been the subject of sustained and arduous controversy for more than a century. Many attempts to resolve the debate have been hampered by a lack of quantitative data. Most of the controversy has centered on three classes of explanations: (1) cotectic crystallization of quartz and plagioclase (*e.g.*, Sugi 1930, Spencer 1938); (2) exsolution of the "Schwantke" component (*e.g.*, Schwantke 1909, Spencer 1945, Phillips 1964, 1973, Hubbard 1966); and (3) metasomatic replacement of the host feldspar (*e.g.*, Becke 1908, Sederholm 1916, Barker 1970). In addition to evaluating these possibilities, we also introduce and discuss two other

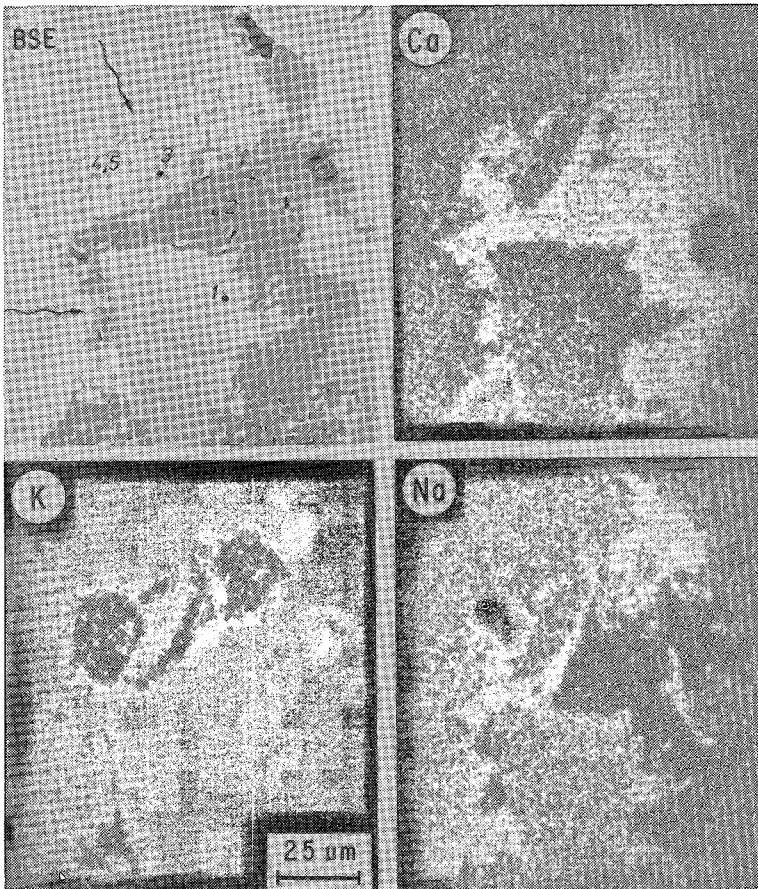


FIG. 13. BSE and X-ray images of intergranular albite-rich area in sample STU 24-21; numbered points correspond to compositions listed in Table 6.

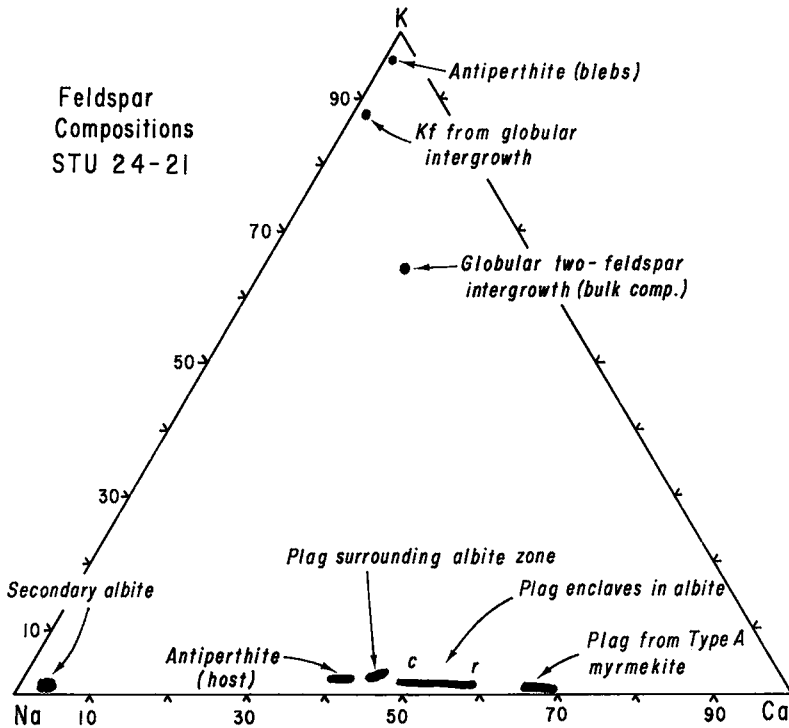


FIG. 14. Summary of feldspar compositions in sample STU 24-21.

hypotheses: (1) isochemical breakdown of a pyroxene precursor, and (2) exsolution of minor-element components.

Cotectic crystallization

In order to test the hypothesis that myrmekite can form by simple cotectic crystallization of plagioclase and quartz, the bulk compositions of myrmekites from St-Urbain have been plotted on a liquidus diagram for the system albite-anorthite-quartz-water at $P(\text{H}_2\text{O}) = 5$ kbar (Fig. 15, Yoder 1968b). The quartz + plagioclase cotectic does not pass through the bulk compositions of myrmekite. This observation argues against the formation of these myrmekites by simple cotectic crystallization. It is unlikely that the small amounts of K and other minor constituents of the myrmekite could shift the cotectic by a sufficient amount so that it would pass through the bulk compositions of the myrmekite. It is also unlikely that variations in total pressure or water pressure could produce the required shift of the cotectic.

Breakdown of a precursor phase

The curious vermicular texture of the type-A inter-

growths is not unlike that produced by eutectoid decomposition in many metal-alloy systems; it also resembles certain examples of exsolution-inversion textures observed in pigeonitic clinopyroxene. Hence, it seems worthwhile to evaluate whether the St-Urbain myrmekites could represent the products of isochemical breakdown of some precursor phase.

As noted earlier, the bulk compositions (Table 3) yield $\text{Si}/\text{O} \approx 0.333$, which corresponds to the $(\text{SiO}_3)_n$ stoichiometry of pyroxene. Accordingly, recalculation of the myrmekite, for example, in sample STU 22-25, as a "pyroxene" (on the basis of 6 oxygen atoms) yields the formula $\text{Na}_{0.091}\text{Ca}_{0.462}\square_{0.451}\text{Al}_{0.996}\text{Si}_{2.000}\text{O}_6$, which corresponds to 90.2 mole % of the Eskola-component ($\square_{0.5}\text{Ca}_{0.5}\text{AlSi}_2\text{O}_6$), 9.1 mole % Jadeite and 0.7 mole % Wollastonite. The other bulk-compositions yield similar results, although they may contain a few mole % of a Tschermak component (CaAlSiAlO_6) in addition.

Evaluation of these data by an alternative method is shown in Figure 16, where bulk compositions have been plotted in terms of relative mole % SiO_2 , $\text{NaAlSi}_2\text{O}_6$ and CaAlSiAlO_6 , using the following conversions: $\square\text{Si}_4\text{O}_8 = 4 \text{SiO}_2$; $\text{CaAl}_2\text{Si}_2\text{O}_8 = \text{CaAlSiAlO}_6 + \text{SiO}_2$; $\text{NaAlSi}_3\text{O}_8 = \text{NaAlSi}_2\text{O}_6 + \text{SiO}_2$. The data points cluster near the line connecting

Eskola pyroxene with Jadeite, which represents the locus of compositions with $Si/O = 0.333$, and passes through the plagioclase field at An_{33} .

These intriguing results are difficult to reconcile with experimental constraints on stability relations for pyroxene. It is well known that the stability field of jadeitic clinopyroxene is restricted to high pressure (e.g., Birch & Lecompte 1961). Recent experimental work on the system $CaO-MgO-Al_2O_3-SiO_2$ at 25–30 kbar has yielded clinopyroxene with 20–26 mole % of the Eskola-component (Wood & Henderson 1978, Gasparik & Lindsley 1980), whereas Smyth (1980) has reported up to 17 mole % of the Eskola-component in kimberlitic omphacite. The pressures indicated from these studies are inconsistent with the geological setting of the St-Urbain massif.

It has been suggested that exsolution lamellae of plagioclase found in orthopyroxene megacrysts at St-Urbain formed as a consequence of *metastable* incorporation (and subsequent decomposition) of a few mole % of the Eskola-component (Dymek & Gromet 1984). However, in the present case, it seems unrealistic to propose the prior existence of a pyroxene with composition $Jd_{10}Esk_{90}$. Consequently, it is

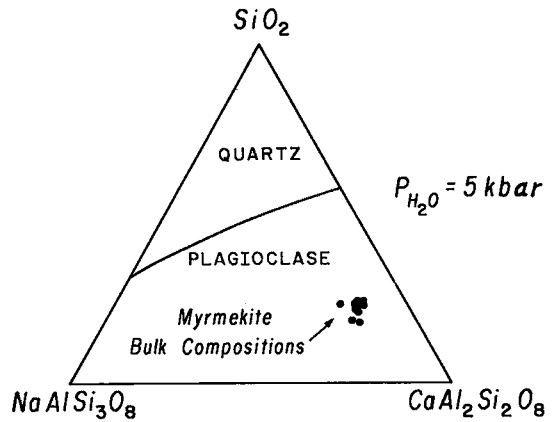


FIG. 15. Bulk compositions of type-A myrmekites plotted on a liquidus diagram for the system An-Ab-Or-H₂O.

unlikely that the St-Urbain myrmekites formed by the isochemical breakdown of pyroxene because the data seem to require a rather preposterous composition for the precursor phase.

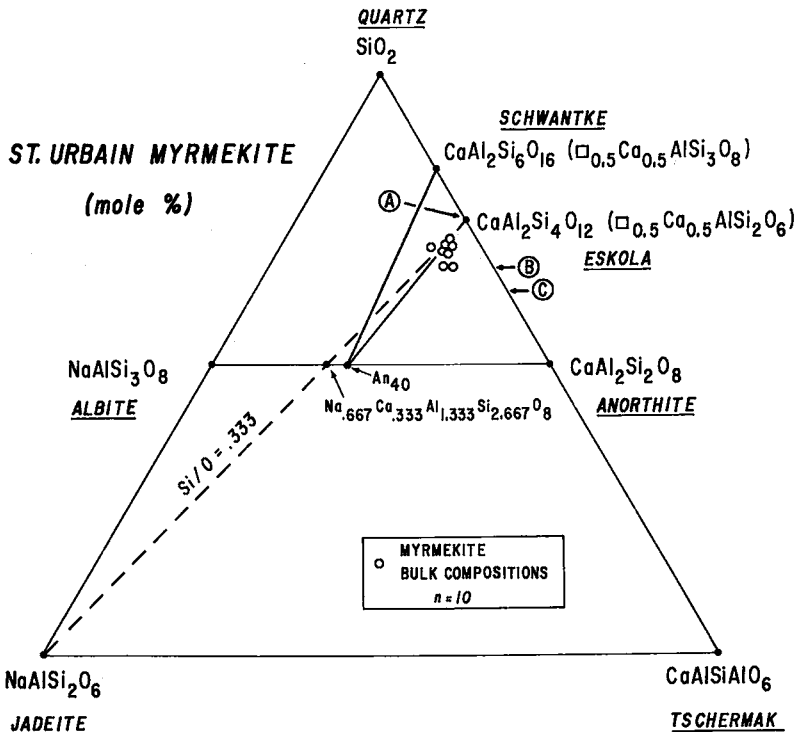


FIG. 16. Bulk compositions of type-A myrmekites plotted in terms of relative mole % $SiO_2-NaAlSi_2O_6-CaAlSiAlO_6$ (see text for discussion).

Exsolution of minor-element components

The presence of abundant blebs of K-feldspar and oriented needles of oxide in the plagioclase indicates that exsolution has been an important process in modifying its original magmatic composition. Moreover, it is possible that some of the tiny inclusions of clinopyroxene in the plagioclase are also of exsolution origin. Therefore, it is important to consider whether the exsolution of K-feldspar, Fe-Ti oxide and, possibly, clinopyroxene may be coupled in some way to the production of myrmekite.

The substitution of potassium into plagioclase represents simple KNa_{-1} exchange that maintains feldspar stoichiometry. Subsequent exsolution of K-feldspar also preserves stoichiometry, but may be inhibited somewhat kinetically as it involves unmixing of (AlSi_3) domains from $(\text{Al}_{1.4}\text{Si}_{2.6})$, which would necessitate some reordering on tetrahedral sites. Nevertheless, we see no reason why the development of myrmekite should be related to the formation of antiperthite.

A full grasp of the implications of oxide or pyroxene exsolution, however, is hampered by a lack of understanding of the precise substitutional relationships for Mg, Fe and Ti in plagioclase as well as uncertainty in the original valence-state of iron. Despite these problems, it is possible to formulate a variety of stoichiometric end-member feldspar components involving simple or coupled Fe, Mg, Ti exchange on anorthite. These are listed in Table 7, together with suggested breakdown-products. Reaction (1) produces clinopyroxene + quartz, (2) produces orthopyroxene + aluminosilicate, (3) produces Fe-Ti oxide + wollastonite + quartz, and

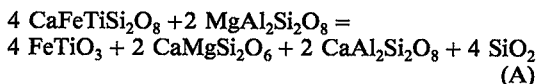
TABLE 7. SOME POSSIBLE MINOR-ELEMENT SUBSTITUTIONAL RELATIONSHIPS FOR ANORTHITE ($\text{CaAl}_2\text{Si}_2\text{O}_8$)

	EXCHANGE	END-MEMBER	DECOMPOSITION PRODUCTS
(1a)	$\text{Fe}^{2+}\text{SiAl}_{-2}$	$\text{CaFeSi}_3\text{O}_8$	$\text{CaFeSi}_2\text{O}_6 + \text{SiO}_2$
(1b)	MgSiAl_{-2}	$\text{CaMgSi}_3\text{O}_8$	$\text{CaMgSi}_2\text{O}_6 + \text{SiO}_2$
(2a)	$\text{Fe}^{2+}\text{Ca}_{-1}$	$\text{FeAl}_2\text{Si}_2\text{O}_8$	$\text{FeSiO}_3 + \text{Al}_2\text{SiO}_5$
(2b)	MgCa_{-1}	$\text{MgAl}_2\text{Si}_2\text{O}_8$	$\text{MgSiO}_3 + \text{Al}_2\text{SiO}_5$
(3a)	$\text{Fe}^{2+}\text{TiAl}_{-2}$	$\text{CaFeTiSi}_2\text{O}_8$	$\text{FeTiO}_3 + \text{CaSiO}_3 + \text{SiO}_2$
(3b)	$\text{Fe}^{3+}_2\text{Al}_{-2}$	$\text{CaFe}_2\text{Si}_2\text{O}_8$	$\text{Fe}_2\text{O}_3 + \text{CaSiO}_3 + \text{SiO}_2$
(4)	$\text{Ti}_2\text{Si}_{-2}$	$\text{CaAl}_2\text{Ti}_2\text{O}_8$	$2 \text{TiO}_2 + \text{CaAl}_2\text{O}_4$
(5)	$\text{Fe}^{2+}\text{TiCa}_{-1}\text{Si}_{-1}$ [=(2b)+1/2(4)]	$\text{FeAl}_2\text{SiTiO}_8$	$\text{FeTiO}_3 + \text{Al}_2\text{SiO}_5$
(6)	$\text{Fe}^{2+}\text{Ti}_2\text{Ca}_{-1}\text{Si}_{-2}$ [=(2b)+(4)]	$\text{FeAl}_2\text{Ti}_2\text{O}_8$	$\text{FeTiO}_3 + \text{TiO}_2 + \text{Al}_2\text{O}_3$ (or $2 \text{TiO}_2 + \text{FeAl}_2\text{O}_4$)
(7)	$\text{MgTi}_2\text{Ca}_{-1}\text{Si}_{-2}$ [=(2a)+1/2(4)]	$\text{MgAl}_2\text{Ti}_2\text{O}_8$	$2 \text{TiO}_2 + \text{MgAl}_2\text{O}_4$ (or $\text{MgTiO}_3 + \text{TiO}_2 + \text{Al}_2\text{O}_3$)

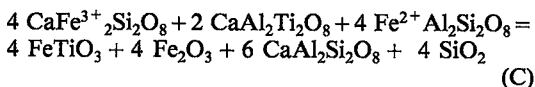
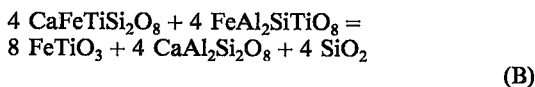
(4) produces rutile + calcium aluminate. Linear combinations of (1) through (4) can be devised that yield a variety of additional products of exsolution, such as Fe-Ti oxide + aluminosilicate (5), ilmenite + rutile + corundum (6), and rutile + spinel (7). As a consequence of all of these reactions, the resultant feldspar is nonstoichiometric (unless the other phases precipitate in addition to pyroxene and oxide).

In the present case, we have not been able to identify exsolution products other than Fe-Ti oxide and K-feldspar (and possibly pyroxene). Moreover, the data on the St-Urbain plagioclases yield stoichiometric proportions of cations, within the limits of analytical error. Therefore, these simplified exsolution-reactions do not seem capable of forming the calcic myrmekites. [Other investigators have identified sillimanite (Sturt 1970) and spinel (Whitney 1972) inclusions possibly of exsolution origin in plagioclase, and it may turn out that information on minor-element substitutions in feldspar can be gained from observations on exsolution products.]

An additional possibility is that these putative exsolution-reactions are coupled in a complex way. For example, a reaction of the type:



provides a convenient mechanism for producing ilmenite, clinopyroxene, plagioclase and quartz by decomposition-exsolution of minor-element components. Production of ilmenite (\pm hematite), plagioclase and quartz (without clinopyroxene) can be accommodated by the following reactions:



Given "appropriate" circumstances, the plagioclase + quartz produced in (A), (B) and (C) could combine to yield myrmekite.

The above reactions have been balanced deliberately such that the products contain 4 SiO_2 in each case. The combination of 4 SiO_2 + 1 $\text{CaAl}_2\text{Si}_2\text{O}_8$ (4 Qtz + 1 An) yields $\text{CaAl}_2\text{Si}_6\text{O}_{16}$ (or 2 $[\square_{0.5}\text{Ca}_{0.5}\text{AlSi}_3\text{O}_8]$, which corresponds to the feldspar "molecule" of Schwantke (1909). As discussed by Phillips (1974), breakdown of the Schwantke

component represents the most commonly cited mechanism proposed for the origin of myrmekite by previous investigators. This model is considered in more detail in the following section.

Exsolution of the Schwantke component

Most discussions of the Schwantke component make the assumption that all the Ca present in the original feldspar phase occurred in the Schwantke "molecule" (e.g., Phillips *et al.* 1972). This assumption restricts the original feldspar to the Ab-Or-Schwantke plane in composition space. An even more restrictive assumption has been applied in some cases, where compositional variation is limited to the Ab-Schwantke binary join. Under these assumptions, complete breakdown of the Schwantke "molecule" would lead to the formation of myrmekite whose quartz content is proportional to its plagioclase composition (Phillips 1964). A number of investigators (Hubbard 1969, Phillips & Ramson 1968, Ramson & Phillips 1969, Shelley 1969, Ashworth 1972, 1973) have noted such a correlation, which they interpret as supporting decomposition of the Schwantke "molecule".

A curve having this form appears on Figure 17 (labeled An₀), which does not pass through the bulk compositions of the St-Urbain myrmekites. Moreover, these bulk compositions do not lie anywhere near a line (not drawn) between "Albite" and "Schwantke" in Figure 16, nor do they lie on the line between "Schwantke" and An₄₀ (observed composition of the host plagioclase in the St-Urbain samples). These features provide strong evidence that the St-Urbain myrmekites did not form by exsolution or decomposition of a feldspar in the Ab-Schwantke-(Or) plane or on the An₄₀-Schwantke join.

The Schwantke "molecule" can be thought of as a feldspar component related to albite by Na₂□Ca exchange or to anorthite by Ca₁Al₂□Si₂ exchange. The first case was discussed above, whereas the latter essentially represents solid solution of "excess silica" in plagioclase.

The suggestion that excess silica occurs in feldspar has been objected to strenuously by many workers (e.g., Orville 1972), but at least two recent experimental studies have demonstrated substantial solubility of Si₄O₈ in CaAl₂Si₂O₈ (up to 17 wt.%; Bruno & Facchinelli 1974, Longhi & Hays 1979). It

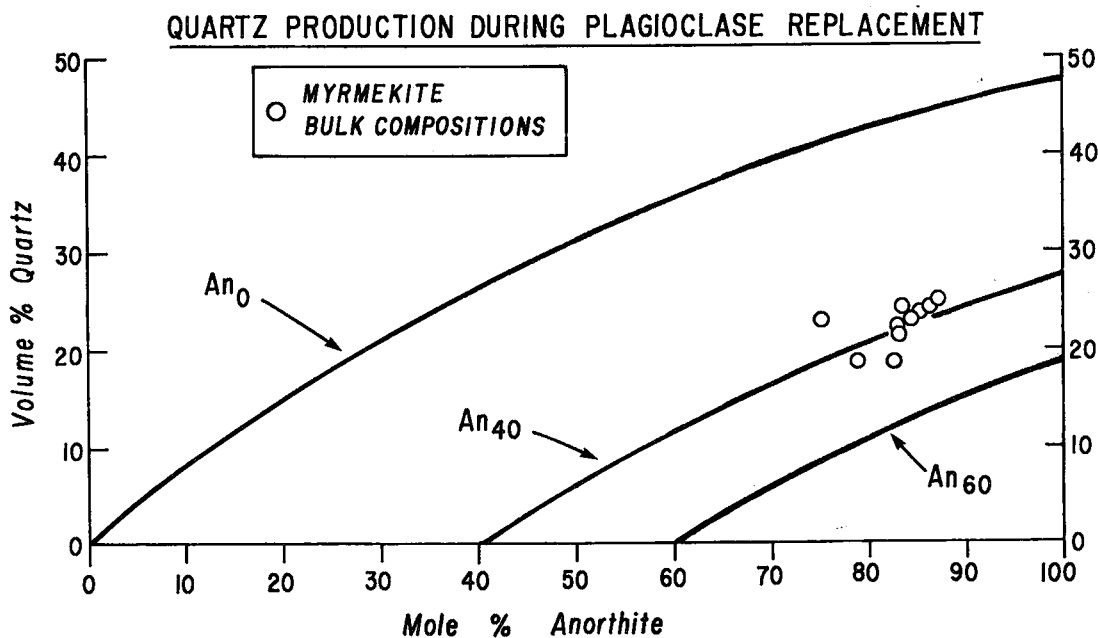


FIG. 17. Bulk composition of St-Urbain type-A myrmekites plotted in terms of volume % quartz versus mole% anorthite. The labeled curves illustrate the relationship between the amount of quartz produced and change in feldspar composition during progressive replacement of sodic by calcic plagioclase, assuming conservation of Al. Note that the curve for An₄₀, which represents the initial composition of St-Urbain plagioclase, passes through the cluster of data points corresponding to the bulk composition of the myrmekite. The curve for An₀ corresponds numerically to breakdown of the Schwantke component and bears no relationship to the present data-set (see text for discussion).

is conceivable therefore that solid solution of Si_4O_8 in plagioclase forms a continuous series of compounds, with the Schwantke "molecule" representing the limit of such solid solutions. Plagioclase in lunar mare basalts appears to contain abundant excess silica (Weill *et al.* 1970, Crawford 1973), but we are unaware of any unequivocal examples of naturally occurring terrestrial plagioclase with excess silica. [Previously, Carman & Tuttle (1963, 1967) had reported excess silica in alkali feldspar and speculated on its bearing to the myrmekite problem, but this interesting study has not been followed up with additional quantitative analytical data.]

In the previous section, we discussed how the coupled exsolution-reactions yield anorthite in excess of that needed to make the Schwantke component; the corresponding silica/anorthite proportions from (A), (B) and (C) are indicated by the arrows on Figure 16. We note that the bulk compositions of the myrmekites are contained within the triangle An_{40} - Anorthite - Schwantke, and lie close to the line from An_{40} to Eskola. Moreover, the silica/anorthite proportions from reaction (A), which involved the exsolution of clinopyroxene, are precisely those of the Eskola-component.

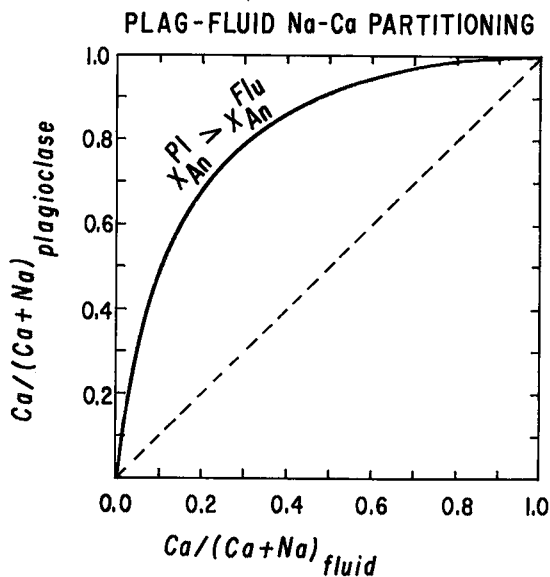
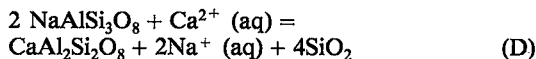


FIG. 18. Schematic representation of an "infiltration isotherm" for a plagioclase - aqueous chloride solution, based on results of Orville (1972). As discussed by Hofmann (1972), the fact that the "isotherm" is concave toward fluid composition indicates that interaction between sodic plagioclase and aqueous fluid will yield calcic plagioclase (and quartz), and that the replacement will tend toward the development of a self-sharpening reaction front. These predictions are consistent with our observations on the St-Urbain myrmekite.

We have remarked earlier that all clinopyroxene inclusions in plagioclase are surrounded by a "halo" showing reverse zoning. These relationships suggest a scenario whereby exsolution of Fe-Ti oxides and clinopyroxene produced silica and anorthite, some of which combined in proportions approximating the Eskola-component (that precipitated along grain boundaries as myrmekite), while the remaining anorthite produced local reversed zoning in the vicinity of the pyroxene. However, this model requires a modal abundance of ("exsolved") clinopyroxene far in excess of the observed amount (some samples contain essentially none). It also requires that the original feldspar contain at least 1 wt.% each of FeO and TiO_2 (based on trial calculations) in order to make the requisite amount of exsolved ilmenite; such values are higher by a factor of 2-3 than those found in bulk compositions of St-Urbain feldspar (Dymek, unpubl. results). Although it is possible that some type of exsolution process has contributed to the development of reverse zoning in the plagioclase, we see no way of linking the formation of myrmekite to exsolution or to any theoretical formulation of the Schwantke component.

Replacement

The nature of the boundary between myrmekite and host plagioclase is strongly suggestive of a reaction front at which An_{40} was converted to An_{80} concomitant with the precipitation of quartz. In our opinion, some type of replacement process involving corrosive interaction between "cumulate" plagioclase crystals and either a late-stage aqueous fluid or water-rich intercumulus melt provides the best explanation for the origin of the St-Urbain myrmekite. Such a replacement process can be modeled in terms of the simplified end-member reaction:

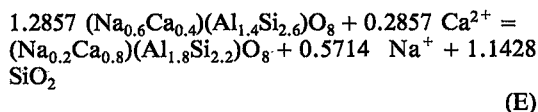


in which the products (calcic plagioclase and quartz) combine to form myrmekite.

Equilibrium conditions for cation-exchange equilibria between plagioclase and aqueous chloride solutions have been determined by Orville (1972; see additional discussion by Wyart & Sabatier 1974, and Helgeson 1974), who also established that reaction (D) proceeds rapidly in the quartz-producing direction but slowly in the quartz-consuming direction. The plagioclase involved in reaction (D) will change composition by coupled $\text{CaAlNa}_{-1}\text{Si}_{-1}$ exchange. We choose to consider the case where Al is conserved in the replacement reaction. This is consistent with experimental data (Orville 1972), and with the obser-

vation that Al is a relatively immobile element in most hydrothermal systems.

The model reaction can be applied to the St-Urbain myrmekite by "adjusting" the compositions of the reactant and product plagioclase to the values observed in our samples (*cf.* Pavlov & Karskii 1949). Accordingly, the conversion of andesine (An₄₀) to bytownite (An₈₀) + quartz can be expressed as:



The relative proportions of the products are fixed by the stoichiometry of reaction (E). The molar ratio of silica to calcic plagioclase corresponds to 20.5 vol. % quartz (if all the silica is precipitated as quartz). This value is in close agreement with the observed amount of quartz in the St-Urbain myrmekites (Table 3). We consider this agreement to be substantial support in favor of a replacement origin for the myrmekite.

The replacement process can be viewed as a continuous reaction that raises the anorthite content of the plagioclase and produces quartz. The proportion of quartz increases as the reactant plagioclase is progressively replaced by an increasingly calcic product. Figure 17 shows the proportionality relationship for three different starting compositions of plagioclase. The curves labeled An₀ and An₆₀ are for reference only; none of the data points plots near these curves. The curve for An₄₀, which corresponds to the composition of the reactant plagioclase at St-Urbain, passes through the cluster of data points representing the bulk compositions of the St-Urbain myrmekites. This confirms that the theoretical replacement-reaction (D) can account for the relative proportions of quartz and plagioclase, as well as the plagioclase compositions that are observed in the St-Urbain myrmekites. It should be evident from Figure 17 that an infinite family of curves, corresponding to a reactant plagioclase of any composition, could be calculated for the replacement reaction.

Two important observations that remain to be explained are: (1) the extremely sharp contact between the myrmekites and plagioclase of their host; and (2) the relatively uniform composition of plagioclase on either side of the contact (with the exception of rare relict "islands" of host plagioclase within the myrmekite). The contrast in plagioclase compositions may indicate that the replacement reaction occurred at conditions where a two-feldspar solvus was intersected. However, the observed plagioclase compositions are not compatible with two

recent (and slightly different) determinations of sub-solidus phase-relations (Grove *et al.* 1983, Smith 1983). We contend that our observations are best explained by the chromatographic theory of infiltration metasomatism (Hofmann 1972). An infiltration process involving reaction (D) has been proposed to explain the origin of myrmekite and reverse zoning of plagioclase in the Bushveld Complex (Schiffries 1982).

A distinctive characteristic of infiltration metasomatism is the occurrence of "plateaus" in the composition of a mineral solid-solution (Hofmann 1972). The plateaus are separated by reaction fronts that may be either sharp or diffuse, depending on the shape of the ion-exchange isotherm (the locus of equilibrium compositions for coexisting mineral and fluid at a given temperature). Experimental data (Orville 1972) for cation-exchange equilibria between plagioclase and aqueous chloride solutions demonstrate that the ion-exchange isotherm for this system is strongly concave toward the fluid composition (Fig. 18), and therefore the reaction front should be self-sharpening (Hofmann 1972). This is consistent with the occurrence of extremely sharp contacts between the plagioclase of the myrmekites and plagioclase of their hosts at St-Urbain.

There is no requirement that the infiltrating fluids be concentrated chloride brines. Orville (1972) showed that the curvature of the infiltration isotherm becomes greater as the chloride concentration of the fluid decreases. The end-member case for "pure" water was studied by Adams (1968), who determined that intermediate plagioclase undergoes incongruent dissolution to anorthite and silica. Thus the infiltrating fluids may have been very dilute: small quantities of magmatically derived water would probably suffice.

Another possibility is that the infiltrating fluid was a silicate liquid rather than a hydrothermal solution. In principle, the effects of magmatic infiltration-metasomatism are analogous to those of hydrothermal infiltration-metasomatism (Irvine 1980). A difficulty with this possibility, however, lies in generating a silicate liquid that would be in equilibrium with both calcic plagioclase and quartz.

However, a replacement origin involving igneous crystallization may be related to the effects of H₂O on the melting behavior of plagioclase feldspars. Figure 19 illustrates a schematic isothermal section in the system An-Ab-H₂O, which will serve as the framework for the ensuing discussion. Initially, the anorthosites consisted of abundant cumulus plagioclase (Pl₁) and a small amount of intercumulus melt (L₁), and contained only an infinitesimal quantity of water (bulk composition given by X). As the water content increases, the bulk composition would move along a line radial to H₂O. The silicate melt migrates isothermally from L₁ toward L₄, dur-

ing which time it would be in equilibrium with progressively more calcic plagioclase (*i.e.*, Pl_1 to Pl_4). Note that a discrete vapor phase would appear only after sufficient H_2O has been added, such that the bulk composition intersects the Plag + Melt + Vapor field (alternative paths and geometries could be constructed such that the melt field could be intersected first).

The increase in water content could be brought about by the progressive crystallization of anhydrous minerals, or by the introduction of external water. In either case, the net result of the above is that increases in H_2O result in corrosion of previously formed plagioclase. This would be a silica-producing reaction if aluminum is conserved in the plagioclase. Although there are strong reasons for advocating Al conservation for the case of hydrothermal replacement, the evidence is less compelling for the case of magmatic replacement. If silica is not precipitated, then this scenario may provide a partial explanation for the abundant reverse zoning observed in some plagioclase. The juxtaposition of An_{40} and An_{80} may signal the instantaneous appearance of an aqueous fluid phase.

SUMMARY, CONCLUSIONS AND PROPOSALS FOR FUTURE STUDIES

The results presented in the previous sections lead to the following scenario for the development of calcic myrmekite in andesine anorthosite from the St-Urbain massif: 1) accumulation of plagioclase crystals (An_{40}) together with minor pyroxene and ilmenite - hematite solid solution from a water-bearing anorthositic magma of unspecified bulk-composition; 2) compaction and upward movement of this cumulate pile as a crystal mush, resulting in the protoclastic development of a seriate porphyritic texture in anorthosites and banded structure in border leuconorites; 3) adcumulus growth of plagioclase concomitant with crystallization of trapped melt to produce additional ilmenite - hematite solid solution, orthopyroxene, clinopyroxene, *etc.*, leading ultimately to the evolution of an aqueous fluid localized at grain boundaries; 4) replacement of An_{40} plagioclase by this fluid, resulting in the widespread formation of calcic myrmekite, and 5) migration of Na-enriched fluid which, upon cooling, caused localized "albitization" (*e.g.*, sample

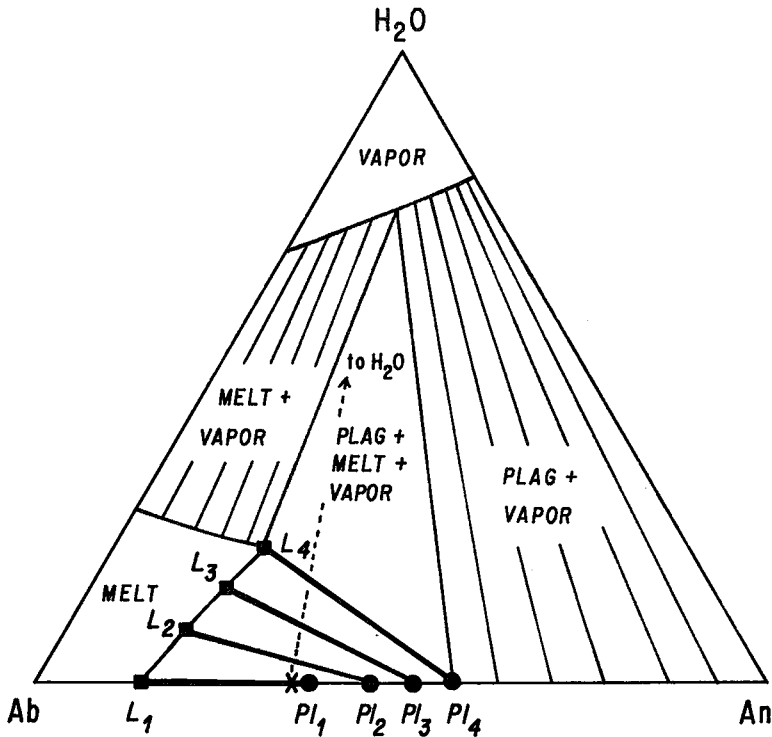


Fig. 19. Schematic representation of the ternary system An-Ab- H_2O ; progressive increase in H_2O -content could cause feldspar resorption or reverse zoning, whereas instantaneous appearance of a separate fluid phase would cause a "jump" in the composition of equilibrium plagioclase from Pl_1 to Pl_4 (see text for additional discussion).

STU 24-21).

A further consequence of the presence of small amounts of an interstitial aqueous fluid is that it could have assisted in the "hydraulic" fracturing of older labradorite anorthosite wall-rock, while it acted as a grain-boundary "lubricant" during the emplacement of anorthositic dykes and veins.

At present, we are unable to specify either the quantity and composition of fluid involved or the temperatures at which the myrmekites formed; stable-isotope studies are planned that may assist in these areas. Direct evidence of an aqueous fluid at some stage in the evolution of the St-Urbain massif is preserved in the form of two-phase (liquid-vapor) fluid inclusions found in interstitial quartz from several samples of andesine anorthosite. Regrettably, the grain size of quartz in the myrmekites is generally too fine to recognize fluid inclusions even if they are present. Nevertheless, the search for fluid inclusions and their characterization assume high priority in view of our postulates for the origin of the myrmekite. Data on homogenization temperatures, salinity, etc., will enable us to assess the role of fluids in a more quantitative fashion.

ACKNOWLEDGEMENTS

This research was supported in part by NSF grant EAR82-06741 to RFD. We thank L.P. Gromet for numerous discussions, S.A. Morse for suggesting the use of the ternary system An-Ab-H₂O as a means of evaluating the effects of water on magmatic plagioclase, and R.B. Hargraves for providing access to several suites of anorthosite samples in order to search for other examples of myrmekite. In addition, we thank Miss Inna Feldman for providing a translation of the paper by Pavlov & Karskii, Mrs. Freda Sofian for typing the manuscript, and two anonymous reviewers for their comments on an earlier version of the paper. Finally, we are especially grateful to R.F. Martin for his thoughtful and comprehensive editing, and for encouraging publication of our data which, we hope, will aid other investigators of anorthosites in general and the myrmekite problem in particular.

REFERENCES

- ADAMS, J.B. (1968): Differential solution of plagioclase in supercritical water. *Amer. Mineral.* **53**, 1603-1613.
- ALBEE, A.L., QUICK, J.E. & CHODOS, A.A. (1977): Source and magnitude of errors in "broad-beam analysis" (DBA) with the electron probe. *In* Lunar Science VIII. The Lunar Science Institute, Houston, 7-9 (ext. abstr.).
- ANDERSON, A.T., JR. (1966): Mineralogy of the Labrieville anorthosite, Quebec. *Amer. Mineral.* **51**, 1671-1711.
- ASHWAL, L.D. (1982): Mineralogy of mafic and Fe-Ti oxide-rich differentiates of the Marcy anorthosite massif, Adirondacks, New York. *Amer. Mineral.* **67**, 14-27.
- ASHWORTH, J.R. (1972): Myrmekites of exsolution and replacement origins. *Geol. Mag.* **109**, 45-62.
- (1973): Myrmekites of exsolution and replacement origins - a discussion. *Geol. Mag.* **110**, 77-80.
- BARKER, D.S. (1970): Compositions of granophyre, myrmekite and graphic granite. *Geol. Soc. Amer. Bull.* **81**, 3339-3350.
- BECKE, F. (1908): Über Myrmekit. *Tschermaks Mineral. Petrog. Mitt.* **27**, 377-390.
- BIRCH, F. & LECOMPTE, P. (1961): Temperature-pressure plane for albite composition. *Amer. J. Sci.* **258**, 207-217.
- BRUNO, E. & FACCHINELLI, A. (1974): Experimental studies on anorthite crystallization along the join CaAl₂Si₂O₈-SiO₂. *Soc. Franç. Minéral. Crist. Bull.* **97**, 422-432.
- BUDDINGTON, A.F. (1960): The origin of anorthosite re-evaluated. *Records Geol. Surv. India* **86**, 421-432.
- CARMAN, J.H. & TUTTLE, O.F. (1963): Experimental study bearing on the origin of myrmekite. *Geol. Soc. Amer., Spec. Pap.* **76**, 29 (abstr.).
- & —— (1967): Experimental verification of solid solution of excess silica in andesine from rhyolites. *Geol. Soc. Amer., Spec. Pap.* **115**, 33 (abstr.).
- CARSTENS, H. (1967): Exsolution in ternary feldspars. I. On the formation of antiperthites. *Contr. Mineral. Petrology* **14**, 27-35.
- CRAWFORD, M.L. (1973): Crystallization of plagioclase in mare basalts. *Proc. Lunar Sci. Conf. 4th*, 705-717.
- DYMEK, R.F. (1980): Petrogenetic relationships between andesine anorthosite dikes and labradorite anorthosite wall rock on Mont du Lac des Cygnes, St-Urbain massif, Quebec. *Geol. Soc. Amer., Abstr. Program*, **12**, 419.
- (1981): Reverse zoning in plagioclase from labradorite anorthosite, St. Urbain anorthosite massif, Quebec: retrograde Plag-Pyx reaction? *Geol. Soc. Amer., Abstr. Program* **13**, 444.
- (1984): Sapphirine of possible igneous origin from the St-Urbain anorthosite massif, Quebec. *Trans. Amer. Geophys. Union* **16**, 295 (abstr.).

- _____ & GROMET, L.P. (1984): Nature and origin of orthopyroxene megacrysts from the St-Urbain anorthosite massif, Quebec. *Can. Mineral.* **22**, 297-326.
- EMSLIE, R.F. (1980): Geology and petrology of the Harp Lake complex, central Labrador: an example of Elsonian magmatism. *Geol. Surv. Can., Bull.* **293**.
- GASPARIK, T. & LINDSLEY, D.H. (1980): Phase equilibria at high pressure of pyroxenes containing monovalent and trivalent ions. In *Pyroxenes* (C.T. Prewitt, ed.). *Mineral. Soc. Amer., Rev. Mineral.* **7**, 309-339.
- GROMET, L.P. & DYMEK, R.F. (1980): Evidence for at least two geochemically distinct anorthosite types in the St-Urbain massif, Quebec. *Geol. Soc. Amer., Abstr. Program* **12**, 438.
- _____ & _____ (1981): Petrological and geochemical characterization of the St-Urbain anorthosite massif, Quebec: summary of initial results. In *Workshop on Magmatic Processes of Early Planetary Crusts*. The Lunar and Planetary Institute, Houston, 30-32 (ext. abstr.).
- GROVE, T.L., FERRY, J.M. & SPEAR, F.S. (1983): Phase relations and decomposition relations in calcic plagioclase. *Amer. Mineral.* **68**, 41-59.
- GUANGHONG, XIE (1982): Petrological characteristics of the Damiao anorthosite complex in Hebei Province, China. *Geochemistry* **1**, 369-385.
- HARGRAVES, R.B. (1962): Petrology of the Allard Lake anorthosite suite, Quebec. *Geol. Soc. Amer., Bulletin* **Vol.**, 163-189.
- HELGESON, H.C. (1974): Chemical interactions of feldspars and aqueous solutions. In *The Feldspars* (W.S. Mackenzie & J. Zussman, eds.). Manchester Univ. Press, Manchester, England.
- HOFMANN, A. (1972): Chromatographic theory of infiltration metasomatism and its application to feldspars. *Amer. J. Sci.* **272**, 69-90.
- HUBBARD, F.H. (1966): Myrmekite in charnockite from southwest Nigeria. *Amer. Mineral.* **51**, 762-773.
- _____ (1969): The proportionality of quartz in myrmekite: a contribution to the discussion. *Amer. Mineral.* **54**, 988-989.
- IRVINE, T.N. (1980): Magmatic infiltration metasomatism, double-diffusive fractional crystallization, and adcumulus growth in the Muskox intrusion and other layered intrusions. In *Physics of Magmatic Processes* (R.B. Hargraves, ed.). Princeton Univ. Press, Princeton, New Jersey.
- KAY, S.M. (1977): The origin of antiperthites in anorthosites. *Amer. Mineral.* **62**, 905-912.
- KEHLENBECK, M.M. (1972): Deformation textures in the Lac Rouvray anorthosite mass. *Can. J. Earth Sci.* **9**, 1087-1098.
- LONGHI, J. & HAYS, J.F. (1979): Phase equilibria and solid solution along the join $\text{CaAl}_2\text{Si}_2\text{O}_8\text{-SiO}_2$. *Amer. J. Sci.* **279**, 876-890.
- MARTIGNOLE, J. & SCHRIJVER, K. (1970): Tectonic setting and evolution of the Morin anorthosite, Grenville Province, Quebec. *Bull. Geol. Soc. Finland* **42**, 165-209.
- MAWDSLEY, J.B. (1927): St-Urbain area, Charlevoix District, Quebec. *Geol. Surv. Can., Mem.* **152**.
- MORIN, M. (1956): *Geology of the Labrieville Map Area, Saguenay County, Quebec*. Ph.D. thesis, Laval Univ., Québec, QC.
- MORSE, S.A. (1982): A partisan review of massif anorthosites. *Amer. Mineral.* **67**, 1087-1100.
- ORVILLE, P.M. (1972): Plagioclase cation exchange equilibria with aqueous chloride solution: results at 700°C and 2000 bars in the presence of quartz. *Amer. J. Sci.* **272**, 234-272.
- PAVLOV, N.V. & KARSKII, B.E. (1949): On the myrmekites in certain basic rocks. *Izv. Akad. Nauk SSSR, Ser. Geol.* **5**, 128-133 (in Russ.).
- PHILLIPS, E.R. (1964): Myrmekite and albite in some granites of the New England batholith, New South Wales. *J. Geol. Soc. Aust.* **11**, 49-60.
- _____ (1972): A comment on "Plagioclase cation exchange equilibria with aqueous chloride solution: results at 700°C and 2000 bars in the presence of quartz". *Amer. J. Sci.* **272**, 969-971.
- _____ (1973): Myrmekites of exsolution and replacement origins - a discussion. *Geol. Mag.* **110**, 74-77.
- _____ (1974): Myrmekite - one hundred years later. *Lithos* **7**, 181-194.
- _____ (1980): On polygenetic myrmekite. *Geol. Mag.* **117**, 29-36.
- _____ & RANSOM, D.M. (1968): The proportionality of quartz in myrmekite. *Amer. Mineral.* **53**, 1411-1413.
- _____, _____ & VERNON, R.H. (1972): Myrmekite and muscovite developed by retrograde metamorphism at Broken Hill, New South Wales. *Mineral. Mag.* **38**, 570-578.
- POWELL, J.A., GROMET, L.P. & DYMEK, R.F. (1982): Quartz monzodiorites and oxide-apatite norites marginal to the St-Urbain anorthosite massif: products of liquid immiscibility? *Trans. Amer. Geophys. Union* **63**, 456 (abstr.).

- RANSOM, D.M. & PHILLIPS, E.R. (1969): The proportionality of quartz in myrmekite - a reply. *Amer. Mineral.* **54**, 984-987.
- ROBIE, R.A., HEMINGWAY, B.S. & FISHER, J.R. (1979): Thermodynamic properties of minerals and related substances 298.15 K and 1 bar pressure and at higher temperatures. *U.S. Geol. Surv. Bull.* **1452**.
- RONDOT, R. (1979): Reconnaissances géologiques dans Charlevoix-Saguenay. *Ministère Richesses Naturelles du Québec*, DPV-682.
- ROY, D.W., RONDOT, J. & DYMEK, R.F. (1972): A crypto-explosion structure at Charlevoix and the St-Urbain anorthosite. *24th Int. Geol. Congress (Montreal). Guidebook, Excursion B-06*.
- SALPAS, P.A., HASKIN, L.A. & MCCALLUM, I.S. (1983): Stillwater anorthosites: a lunar analog? *Proc. Lunar Planet. Sci. Conf. 14th, J. Geophys. Res.* **88**, B27-B39.
- SCHIFFRIES, C.M. (1982): The petrogenesis of a platiniferous dunite pipe in the Bushveld Complex: infiltration metasomatism by a chloride solution. *Econ. Geol.* **77**, 1439-1453.
- SCHWANTKE, A. (1909): Die Beimischung von Ca im Kalifeldspat und die Myrmekitbildung. *Centralbl. Mineral.*, 311-316.
- SEDERHOLM, J.J. (1916): On synantectic minerals and related phenomena. *Comm. Géol. Finlande Bull.* **153**.
- SHELLEY, D. (1969): The proportionality of quartz in myrmekite: a discussion. *Amer. Mineral.* **54**, 982-984.
- SHUL-DINER, V.I. (1972): The problem of myrmekites. *Int. Geol. Rev.* **14**, 354-358.
- SPENCER, E. (1938): The potash-soda feldspars. II. Some applications to petrogenesis. *Mineral. Mag.* **25**, 87-118.
- _____ (1945): Myrmekite in graphic granite and in vein perthite. *Mineral. Mag.* **27**, 79-98.
- SMITH, J.V. (1974): *Feldspar Minerals. 2. Chemical and Textural Properties*. Springer Verlag, New York.
- _____ (1983): Phase equilibria of plagioclase. In *Feldspar Mineralogy* (2nd edition, P.H. Ribbe, ed.). *Mineral. Soc. Amer., Rev. Mineral.* **2**, 223-239.
- SMYTH, J.R. (1980): Cation vacancies and the crystal chemistry of breakdown reactions in kimberlitic omphacites. *Amer. Mineral.* **65**, 1185-1191.
- STURT, B.A. (1970): Exsolution during metamorphism with particular reference to feldspar solid solutions. *Mineral. Mag.* **37**, 815-832.
- SUGI, K. (1930): On the granitic rocks of Tsukuba district and their associated injection-rocks. *Jap. J. Geol. Geog.* **13**, 29-112.
- VON GRUENEWALDT, G. (1979): A review of some recent concepts of the Bushveld Complex, with particular reference to sulfide mineralization. *Can. Mineral.* **17**, 233-256.
- WAGER, L.R. & BROWN, G.M. (1968): *Layered Igneous Rocks*. Oliver & Boyd, Edinburgh, Scotland.
- WEILL, D.F., MCCALLUM, I.S., BOTTINGA, Y., DRAKE, M.J. & MCKAY, G.A. (1970): Petrology of a fine-grained rock from the Sea of Tranquility. *Science* **167**, 635-638.
- WHITNEY, J.A. & STORMER, J.C., JR. (1977): The distribution of $\text{NaAlSi}_3\text{O}_8$ between coexisting microcline and plagioclase and its effect on geothermometric calculations. *Amer. Mineral.* **62**, 687-691.
- WHITNEY, P.R. (1972): Spinel inclusions in plagioclase of metagabbros from the Adirondack Highlands. *Amer. Mineral.* **57**, 1429-1436.
- WOOD, B.J. & HENDERSON, C.M.B. (1978): Compositions and unit-cell parameters of synthetic non-stoichiometric tschermakitic clinopyroxenes. *Amer. Mineral.* **63**, 66-72.
- WYART, J. & SABATIER, G. (1974): Can Schwantke's compound be formed by reaction of alkalic feldspars with hydrothermal calcic solution? A comment on the recent paper by P.M. Orville: Plagioclase cation exchange equilibria with aqueous chloride solutions at 700°C and 2000 bars in the presence of quartz. *Amer. J. Sci.* **274**, 633-637.
- YODER, H.S., JR. (1968a): Experimental studies bearing on the origin of anorthosite. In *Origin of Anorthosite and Related Rocks* (Y.W. Isachsen, ed.). *New York State Museum Sci. Serv., Mem.* **18**, 13-22.
- _____ (1968b): Albite-anorthite-quartz-water at 5 Kb. *Carnegie Inst. Wash. Year Book* **66**, 477-478.

Received January 9, 1985, revised manuscript accepted August 25, 1986.